THE JOURNAL OF SOLAR ENERGY SCIENCE AND ENGINEERING

VOLUME I | OCTOBER, 1957 | NUMBER 4

Table of Contents

Page

Solar Energy Collection in the Pacific Northwest 3
Richard W. Crain, Sr.

Plastics for Focusing Collectors 9
J. A. Duffie, R. P. Lappala, and G. O. G. Lof

Concentration of the Solar Radiation in a Solar Furnace 14
Taro Hisada, Hisao Mii, Choji Noguchi, Tetsuo Noguchi, Nobuhei Hukuo, and Masao Mizuno

The Flux through the Focal Spot of a Solar Furnace 19
Paul D. Jose

Heat Flux Measurements at the Sun Image of the California Institute of Technology Lens-Type Solar Furnace 23
Eugene Loh, Nevin K. Hiester, and Thomas E. Tietz

A Guidance System for a Solar Furnace 27
James G. Moore and Pierre St. Amand

Solar Radiation during the Solar Eclipse of December 14, 1955 at Colombo, Ceylon 30
P. Selvanayagam and J. C. V. Chinnappa

Solar Energy in Spain 32
Leonardo Villena

A Survey of Solar Furnace Installations in the United States 35
Supplement

World Research Activities 36

Solar Abstracts 38

Errata & Addenda 40

The cover of this issue shows the solar furnace of the Government Industrial Research Institute at Nagoya, Japan. (See paper page 14.) A Conn-type installation constructed in 1955, this furnace uses a 2-m parabolic reflector of high-purity aluminum plate, with no auxiliary mirror.

VOL.
1
1957

SOLAR ENERGY COLLECTION IN THE PACIFIC NORTHWEST

By RICHARD W. CRAIN, Sr.

Department of Mechanical Engineering, University of Washington, Seattle

The solar energy collection apparatus at the University of Washington has been improved and changed since the original paper on this apparatus was presented by the author in November, 1955. Two different types of collectors are now collecting solar energy, side by side and simultaneously, namely a flat-plate and a parabolic-type collector. Both collectors are attached to a common shaft and fixed so that they will rotate together and track the sun in its travel across the sky. These two collectors can also be changed in inclination to various positions such that the collector surfaces always receive the sun's rays at right angles, for most efficient solar collection. The controls effecting this operation are thoroughly explained in this paper. The efficiency of a collector is the ratio of the energy collected by it to the energy recorded by a pyrheliometer. This efficiency indicates how much of the sun's energy that actually impinges on the earth the collector is capable of absorbing and thus transferring to some medium for future use.

A comparison of the flat-plate and the parabolic collector is made in this paper, along with thorough explanations of all the aspects of the apparatus, illustrated by actual photographs and line drawings. A comparison is also made between fixed collectors and collectors which track the sun. In addition, a comparison is made between the energy that can actually be collected and the energy represented by the total heat loss from an average Seattle home, thus indicating how well the collected solar energy could replace this heat loss, provided the energy could be satisfactorily transferred by an appropriate medium into the house. Finally, mention is made of future research contemplated on solar energy collection and utilization in the Pacific Northwest.

FIG. 1 — Solar energy collector in fixed position.

In November, 1955, the author first presented a paper describing the solar radiation apparatus at the University of Washington at Seattle. This presentation was made at the Technical Session of the Conference on Solar Energy — the Scientific Basis, held at the University of Arizona, Tucson. This paper will be published soon in the transactions of the conference now being prepared. It discusses the thought behind the original design, but the number of actual results given is limited because of the short time the apparatus had been in operation at the time the paper was presented.

Since the writing of the above-mentioned paper, much has been done to improve and to add to this solar radiation apparatus. Improvements and additions have altered the original purpose of the research on this project. Whereas, initially, the project was devised merely to furnish a "data-collecting instrument" in order to determine the amount of useful solar energy that can be made available in the Pacific Northwest, now the purposes of the project are changing to the gathering of more practical and useful information such as means of storage and methods of using the energy collected.

As originally set up,[1] the solar energy collecting apparatus could use but one type of collector at a time and then only in one fixed position. Although this fixed position could be changed at various times of the year to such angles of inclination to the roof top as effectively face the sun, the sun's rays could be perpendicular to the collecting surface only during a very few minutes of each day. Fig. 1 shows a collector in this fixed position. During 1955 to

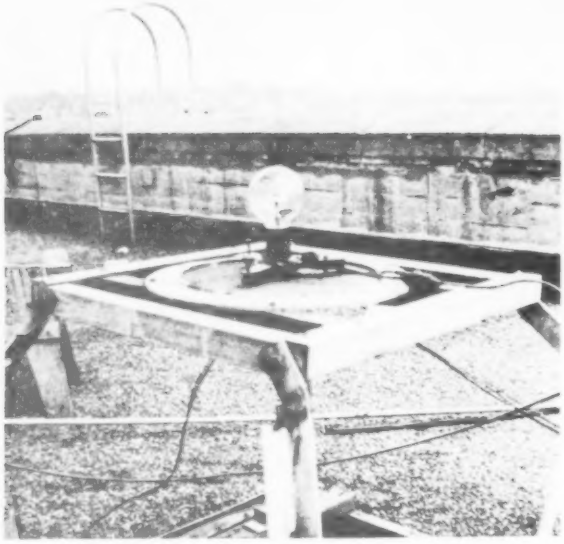

FIG. 2 — Pyrheliometer.

TABLE I
AVERAGE SOLAR HEAT COLLECTED — FIXED POSITION

Month (1955-56)	Average Collected (Btu/day/ft²)	Average Solar Heat Available by Pyrheliometer (Btu/day/ft²)	Efficiency of Collectors (per cent)
June	734	1440	50.8
July	729	1410	51.5
August	1113	1490	74.5
September	729	940	77.5
October	299.7	475	63.0
November	199	303	65.5
December	568	915	62.0
January	243	405	60.0
February	230	396	58.0
March	716	950	75.0
April	945	1490	63.0
May	1023	1620	63.2

1956 (June to May) data were taken on two types[1] of collectors alternately, the collectors being in fixed positions as mentioned above. One type was a flat plate with copper-tubing coils soldered onto the plate surface, all being blackened. The other type was a parabolic type, with copper tubing running along the focal length of each of twelve stainless steel reflectors 3 ft long, placed side by side. The average solar energy collected each month, in Btu per day per sq ft, is shown in Table I. The efficiency of the collector is a comparison of the energy collected to the energy recorded by a pyrheliometer (see Fig. 2). The pyrheliometer is capable of measuring, at its locale, the maximum amount of solar energy which impinges upon the earth.

In comparing the two types of collectors during this period of fixed operation, the flat-plate collector showed a higher average efficiency than the parabolic collector on bright days. However, on dull days, the reverse was true. The following reasons have been concluded from the data collected and analyzed: (1) The reflector collector is the more reliable or constant collector, in that the flat-plate collector has a much larger difference in efficiencies because of sky conditions, its efficiencies overlapping the reflector efficiencies on both the good and poor ends of the scale. (2) The losses causing a drop in efficiencies in the reflector collector are: transmission through the glass, loss due to inefficient reflector, reradiation loss, and conduction out of the box. If operated at the same temperatures, there being no conduction loss in getting the energy to the transfer medium since the energy is applied directly to the tubes, the glass loss and loss from the box will be the same for both collectors. In the flat-plate collector, in addition to the glass and box losses mentioned above, there are conduction losses through the plate to the tubes and reradiation losses. So, considering just the two losses which will be different for each system, the difference in efficiencies can be explained, it seems, by the fact that the losses on the reflector collector remain constant or increase slightly, while the losses on the flat plate increase considerably. (3) Finally, it appears that the reradiation for the flat plate and the plate conduction losses are the key ones, and that the reradiation perhaps is more, proportionately, when reradiating to clouds than when reradiating to the sun on a bright day.

Further analysis of the fixed-collector data gives a comparison of the energy the apparatus can make available from the sun to the heat loss from an average home in Seattle that this solar energy could replace. The average energy collected amounts to 60 Btu per sq ft per hr, which is sufficient to replace the loss from an average home of 12 Btu per sq ft per hr, provided the solar energy collected is satisfactorily stored and efficiently transmitted to the home. From this analysis, the next logical step was to improve the collection of solar energy and devise good

FIG. 3 — Collector inclination on June 21.

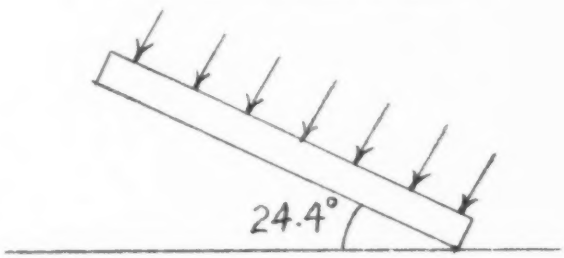

FIG. 4 — Collector inclination on December 21.

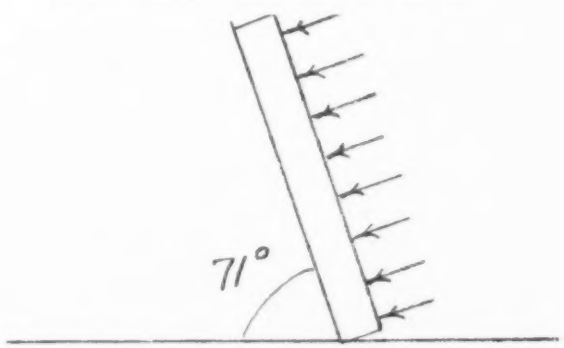

VOL.
1
1957

FIG. 5 — Base section of solar collector frame.

FIG. 7 — Side view of solar energy collection apparatus.

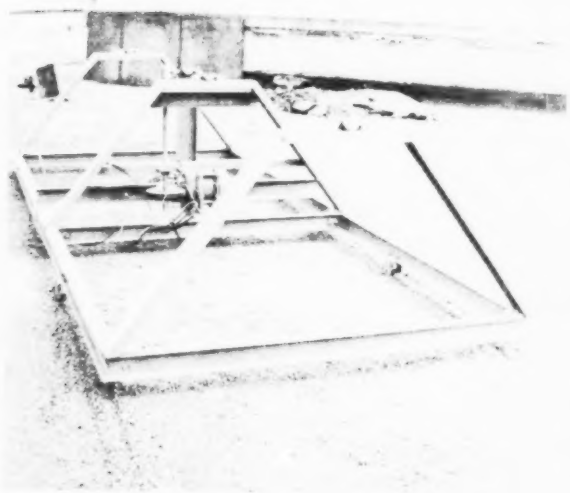

FIG. 6 — Collector stand of solar collector frame.

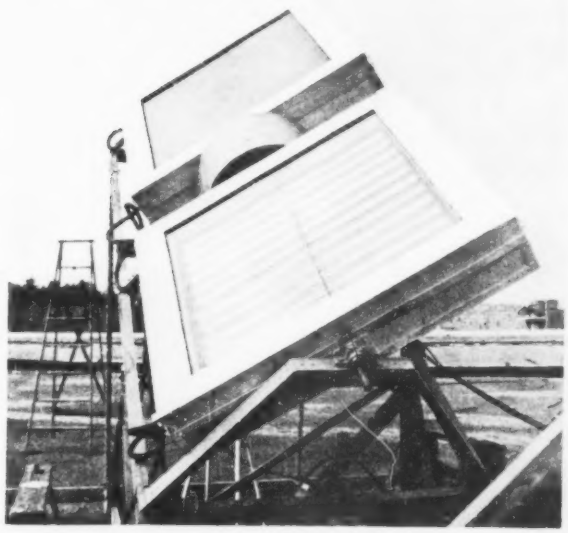

FIG. 8 — Front view of solar energy collection apparatus.

methods of storage, transmission, and use of the energy captured.

To improve the collection of solar energy, the two types of collectors were put into the same framework, end to end, and caused to rotate together and follow the sun during the day by means of an electrically controlled, geared tracking system. The collectors are tipped at an appropriate angle of inclination, which can be varied according to the season of the year. This is done once a month, so that, in conjunction with tracking the sun, the sun's rays are always at right angles to the collectors' surfaces. The sun's extreme northern position is 23°27′ north latitude, whereas Seattle's location is 47°39′ north latitude and 122°18′ west longitude. The sun in Seattle, then, always has a declination between approximate angles of 65.6° and 19°. The complement of the declination of the sun is the angle of inclination of the collector, which, as shown in Figs. 3 and 4, is always between 71° and 24.4°.

The framework for holding the collectors consists of aluminum-alloy extrusions reinforced at the joints with steel. Three basic weldments are bolted together to provide for disassembly, to facilitate transportation, and to make possible the construction indoors. Two basic sections comprise the structure: (1) the base section, shown in Fig. 5, which supports (2), the collector stand shown in Fig. 6, by being mounted to the base by two pillow blocks which have two telescoping tubing supports as a means for changing the elevation or inclination of the collectors.

The collector stand supports the collectors, collector

FIG. 9 — Spindles in pillow blocks.

FIG. 10 — Adjustment for monthly change in collector inclination with horizontal.

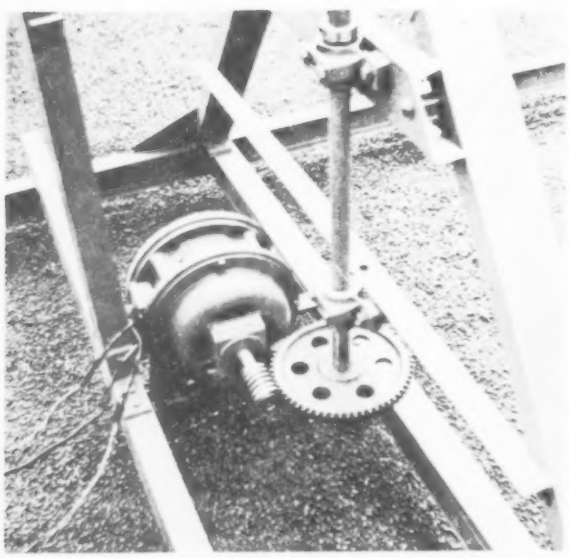

FIG. 11 — Motor and reduction gear for traversing the collectors.

frames, motor, gearing, and other miscellaneous attachments, as shown in Figs. 7 and 8. The collector frames are attached to 1.25-in. diameter spindles supported at four locations by cast iron pillow blocks (Fig. 9). To permit the collector surfaces to remain normal to the sun's rays (with tracking the sun), the angle of inclination which the collector surface makes with the horizontal is adjusted monthly by means of the telescoping tubing supports (Fig. 10). The angle through which the collectors are moved in inclination is an average of about 7.8°, since the sun moves through a total angle of declination from 19° to 65.6° semiannually.

Fig. 11 shows the motor and reduction-gear arrangement for traversing the collectors. The motor at 1735 rpm, 0.75 hp, 3 phase, 220 volts, runs off its shaft a 1.5-in. worm drive, which drives a worm gear of 7.5-in. pitch diameter mounted on a vertical shaft. At the top end of this vertical shaft another 1.5-in worm drives a 12.5-in. pitch diameter worm gear which is installed on the center collector frame spindle. The speed reduction is approximately 6000 to 1 or a final speed of traverse of the collectors of 0.29 rpm.

To traverse the collectors so that the sun's rays remain normal to the collector surfaces, a device consisting of an electric timer and automatic reset switch is used to operate the motor at periodic intervals and to permit rotation of the collectors a given number of degrees each time.

Fig. 12 sets forth the complete circuit which operates and controls the movement of the collectors as they track the sun, and Fig. 13 shows the actual control equipment. The timing device, a Cycle Master time switch, can, through a 110-volt a-c power source, be preset for the desired length of cycle. In Seattle, this length of cycle varies from 8 hours 25 min, the length of time of sun

FIG. 12 — Complete forward and reverse circuits, electric timer sun-tracking control.

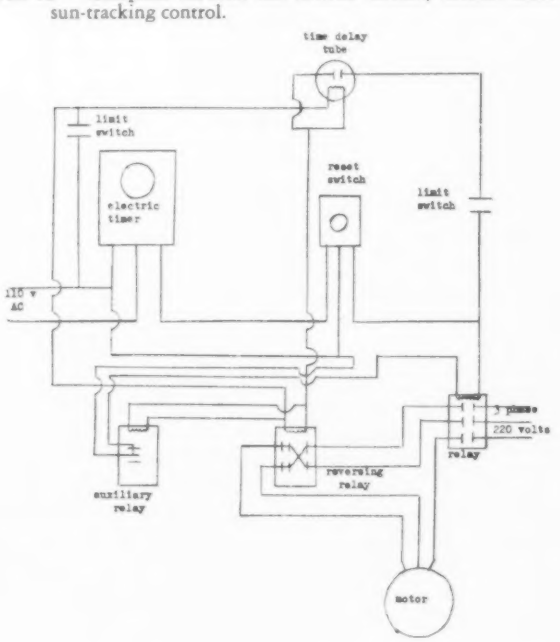

VOL. 1 1957

travel on the shortest day of the year, to 16 hours on the longest day. When the time cycle, which lasts from ¼ to ¾ hour, as shown in Table II, has passed, the timer will deliver a 110 volt a-c voltage to the reset switch. Then a pulse of 0.2 to 0.4 sec automatically closes the relay which allows the 3-phase, 220-volt motor to operate for the length of time of the reset pulse, thus rotating the collectors the required amount to keep the sun's rays perpendicular to them. Table III shows sunrise and sunset times in Seattle.

TABLE II
CONTROL SETTINGS

Length of Day (hours)	(min)	Time Interval (hours)	Reset Time Pulse (sec)
8	25	¼	0.2
10	0	½	0.5
12	0	½	0.3
14	0	½	0.2
16	0	¾	0.4

TABLE III
SUNRISE AND SUNSET TIMES FOR SEATTLE, WASHINGTON

Date	Sunrise (a.m.)	Sunset (p.m.)
Jan. 21	7:24	4:26
Feb. 21	6:37	5:13
March 21	5:49	6:01
April 21	4:55	6:55
May 21	4:13	7:37
June 21	3:54	7:56
July 21	4:11	7:39
Aug. 21	4:54	6:56
Sept. 21	5:47	5:59
Oct. 21	6:36	5:14
Nov. 21	7:24	4:26
Dec. 21	7:44	4:06

FIG. 13 — Control box of sun-tracking control.

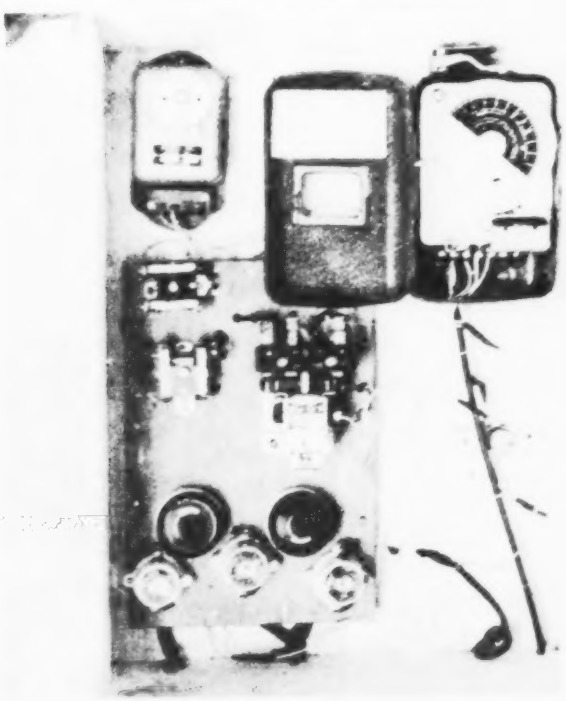

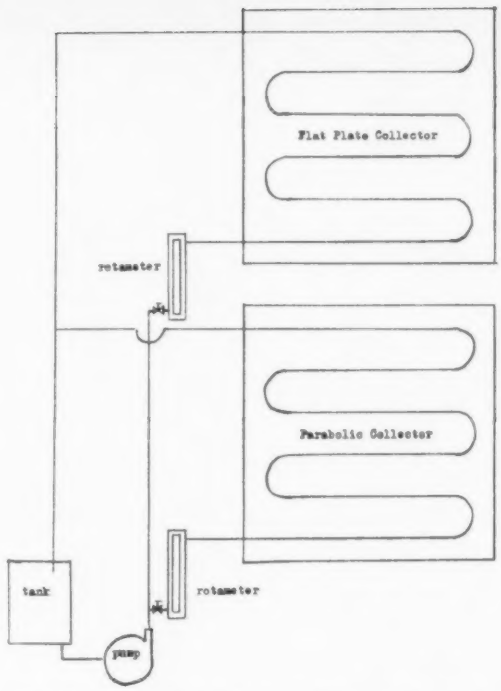

FIG. 14 — Flow diagram for antifreeze in closed circuit.

At the end of each day the collectors are rotated back to position for the following day of operation by means of the reverse circuit, as shown in the complete circuit sketch of Fig. 12. At the end of each day, when the sun sets, the limit switch is actuated in order to direct voltage to the reversing relay and reverse two of the motor leads. To prevent burning of the reversing-relay contact points the time-delay tube is connected across the limit-switch leads and delays the action of the motor relay 30 sec to insure that the reversing-relay contact points have closed before the motor relay. During the reversing operation, the reset switch is disconnected by the auxiliary relay. The reverse rotation of the collectors is stopped at the proper position to start the next day's operation by the second limit switch.

The original heat transfer medium used in this apparatus was water. However, a sudden cold snap caused breakage of part of the piping, rotameter, and valves. The system was therefore converted to a closed system using an antifreeze solution which was pumped from a tank through the collectors and back to the tank as illustrated in Fig. 14.

Copper-constantan thermocouples are used in the water-in and water-out lines of both collectors to obtain the respective temperatures of the circulating medium. These four thermocouples are connected to a Micromax Recorder using a strip chart for recording the various temperatures. To identify the various temperatures, green ink records the temperature of water-in of the flat-plate collector and black ink for the water-out, while red and purple ink record the water-in and water-out temperatures respectively of the parabolic reflector collector. The elec-

TABLE IV

EVALUATION OF COLLECTORS, TRACKING THE SUN

Date (May, 1956)	Pyrheliometer Recording Radiation (cal/day/cm²)	Radiation (Btu/day/ft²)	Flat Plate (Btu/day/ft²)	Parabolic (Btu/day/ft²)	Flat Plate Efficiency (per cent)	Parabolic Efficiency (per cent)
18	674.7	2200	1545	1070	70	52
19	599.1	1598	960	640	61	40
20	425.1	1393	847	692	61	50
21	727.2	2370	1083	920	47	39
22	671.1	2200	2002	1309	91	63
23	433.8	1420	714	553	50	39
24	432.0	1380	1078	665	78	48

tric timer described above automatically sets the Micromax in operation at the beginning of each day's collection and stops it at sundown.

For a short period of time in the spring of 1956, data were collected and efficiencies were calculated to show a comparison of the two types of collectors, flat-plate and parabolic reflectors, as shown in Table IV. Both collectors operated together tracking the sun at the proper inclination for that time of year.

The heat collected by each collector is calculated by this equation, heat expressed in Btu per day per sq ft:

$$Q = \frac{W}{3} \Delta t \, c_p \frac{1}{\text{area}}$$

Q = Btu/day/ft²

W = weight of medium (water or antifreeze) lb/hr

Δt = total temperature difference, temperature medium in to out. (Addition of all average temperature differences during each 20 min period)

c_p = specific heat of medium (1 for water, 0.93 for antifreeze)

area = collector area = 16 ft²

The pyrheliometer collection of solar energy is recorded on a Micromax adjacent to the collectors' Micromax in the same room, directly below the roof where the collector apparatus and pyrheliometer are located side by side. The heat collected by the pyrheliometer is recorded in cal per day per sq cm and is converted to Btu per day per sq ft by a multiplier of 3.685. Then the ratio of heat collected by the solar apparatus to that absorbed by the pyrheliometer gives the efficiency of the collector.

Table IV results indicate an advantage of the flat-plate collector over the parabolic. This would seem to substantiate the previous conclusion above that for fixed operation the flat plate showed the better efficiencies on bright, sunny days. However, this is not entirely conclusive as yet because of the short time the data has been collected. Also, a variation in pressure head of medium to the two collectors would cause some effect. During the summer and fall of 1956, considerable trouble was encountered, necessitating a complete overhaul. As a result, a new circulating tank of larger capacity, new pump, new pipe lines, and a standpipe to equalize pressure conditions for both collectors were installed.

This new apparatus is shown in Fig. 15. At this writing, new data is not ready, but it is hoped that at a later date we will be ready to publish further analyses of these two types of collectors which will be much more reliable and conclusive as a result of continuous and faultless operation for a considerable length of time.

Another future development will also be forthcoming. Preliminary plans and calculations are now underway for the use of the heat collected by this solar apparatus in conjunction with a heat pump installation which is under the supervision of Professor George Smith of the Electrical Engineering Department at the University of Washington.

ACKNOWLEDGEMENTS

The construction and design of this solar apparatus has been done under the supervision of the author, by the following students in Mechanical Engineering at the University of Washington:

Richard W. Crain, Jr.....1954-55
Gordon A. Vincent.....1954-55
Bradley O. Reese.....1955
Fayette Brown.....1955-56
Balwant Singh.....1955-56
Donald Peterson.....1956
Richard L. Lankford.....1956-57
Richard E. Scheumann.....1956-57
Richard D. Burgoon.....1957
Larry D. Krull.....1957

REFERENCES

1. Richard W. Crain, Sr., "A solar radiation apparatus." (To be published in the *Transactions of the Tucson Conference on the Use of Solar Energy — the Scientific Basis*. Tucson, Univ. of Arizona Pr.)

FIG. 15 — Solar energy collecting apparatus at present.

VOL. 1 1957

PLASTICS FOR FOCUSING COLLECTORS

By J. A. DUFFIE*, R. P. LAPPALA**, and G. O. G. LOF***

The use of plastics in fabrication of reflectors for focusing collectors offers possibilities for reduction of material and fabrication costs. Fiber-glass-reinforced polyesters, cellulose acetate butyrate, and polystyrene have been considered for reflector shell fabrication, and vacuum-metallized films for reflecting surfaces. Polystyrene shells with aluminized Mylar reflective lining have been the most promising of the materials considered. Flexible laminates of aluminized Mylar to vinyl or vinyl-cloth combinations are considered for flexible reflectors. Application of plastic reflectors to solar cookers is noted.

INTRODUCTION

Thermal processes for the utilization of solar energy require collectors of flat-plate or focusing types. The choice of a type of collector depends on the temperature required for the particular use and on the economic factors which determine the cost of the collected energy, i.e., the initial cost of the collector, its efficiency, its useful life, etc. This paper is concerned with the problem of materials of construction for reflectors for focusing-type solar collectors and deals with the use of some plastic materials which may make possible some collector cost reduction.

Many focusing solar reflectors have been described in the technical and patent literature. (See Refs. 1 and 2 for bibliographies.) The most common shapes have been the parabola of revolution and the cylindrical parabola. Conical, spherical, and circular cylindrical shapes have also been used. Although fabrication and orientation of the cylindrical types of reflector are simplified by the lack of compound curvatures, higher concentration ratios, i.e., the ratio of projected area of the reflector to the area of the receiver, can be obtained with surfaces of revolution. Forming techniques such as vacuum and drape molding, which are standard practices with some plastic materials, lend themselves to fabrication of the compound curvatures required for such collectors. The use of plastic materials and simple fabrication processes in the production of inexpensive solar reflectors is a logical and practical approach toward the use of solar energy in suitable applications.

*University of Wisconsin.
**University of Wisconsin and Bjorksten Research Laboratories.
***University of Wisconsin and Chemical Engineering Consultant, Denver.

REFLECTOR DESIGN FACTORS

The problems in reflector design and construction can be divided into those involving the reflective linings and those pertaining to the support for the reflective lining, i.e., the reflector shell and its supporting structure.

The efficiency of a focusing solar collector is directly proportional to the specular reflectivity of the reflecting surfaces. The initial specular reflectivity must be acceptably high; it must be capable of maintenance at a high level, or the reflecting material must be inexpensive enough to be renewed at whatever intervals may be required to maintain the desired efficiency. Resistance to weathering, ease of cleaning, and the resistance of the reflective surface or a protective layer to abrasion and solvents, as well as first cost of the materials, are of importance in determining the cost of thermal energy collected with reflectors.

The shells which support the reflective surface and their supporting structures must be fabricated with an accuracy which is dictated by the use to which the focusing collectors will be put. The higher the concentration ratio required, the more precise must be the construction of the reflector shell. For solar cookers and low pressure steam generators, concentration ratios may vary from as low as two to as high as several hundred. Solar furnaces may have theoretical concentration ratios in the range of 35,000 to 50,000 and require a high degree of precision in their manufacture. Good collector efficiency requires dimensional stability sufficient to maintain the desired concentration ratio.

Of particular importance are the costs of the plastic materials, their fabrication, and transportation. Other important factors are the requirements for positioning the unit relative to the sun, the ease of maintenance, and the weight of the units, which affects their transportability, stability, and mobility for positioning. The required accuracy of orientation of the collectors is also a function of the concentration ratio; solar furnaces of high concentration ratio are controlled by photoelectric or clock guidance systems, whereas solar cookers of low concentration ratio may be positioned easily by hand at appropriate intervals.

The materials studies herein reported are illustrated by application to two types of reflective solar cookers, having concentration ratios in the range of 100 to 400. One of the cookers, designed for use primarily by people of non-

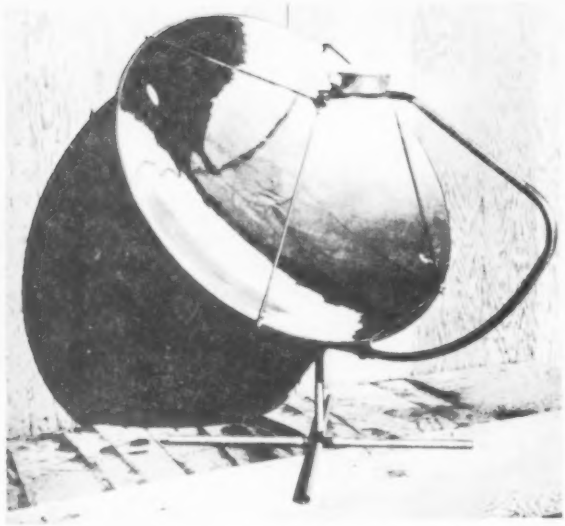

FIG. 1 — The Wisconsin solar cooker, consisting of a mounting frame bent from ¾-in. thinwall tubing and a 50-mil drape-formed high-impact polystyrene reflector shell lined with aluminized Mylar film.

industrialized areas, utilizes a rigid, one-piece parabolic reflector of 18-in. focal length and 43-in. aperture. These dimensions result in the equivalent of approximately 650 watts being reflected to a cooking vessel when the direct incident radiation is 5 Btu per sq ft per min, and the specular reflectivity is 80 per cent. For this cooker, the additional requirements of ease of handling, transportability, and ready cleanability are imposed. Fig. 1 shows a photograph of the Wisconsin solar cooker, which utilizes a simple mounting, manually adjustable for altitude angle and azimuth, and a 50-mil drape-formed high-impact polystyrene shell lined with a reflecting lining of aluminized du Pont "Mylar" polyester film.

The second type of cooker, shown in Figs. 2 and 3, is designed for recreational use. A folding reflector of aluminized Mylar laminated to a vinyl-cloth combination is mounted on an umbrella frame, and the material is so cut and sewn that the cross section of the opened reflector, along the centers of opposite panels, is parabolic. The effective reflectivity of this flexible material is lower than that of the rigidly supported metallized film; at a reflectivity of 70 per cent, a 45-in. reflector will deliver about 660 watts.

EXPERIMENTAL STUDIES

Materials used in the experimental reflector program have been fiberglass-reinforced polyester, high-impact, polystyrene, cellulose acetate butyrate, and laminates of vinyl and cloth for reflector shells; aluminized Mylar and silvered cellulose acetate butyrate have been employed for reflecting surfaces. All of the rigid shells were molded on spun aluminum paraboloids with focal lengths of 18 in. and apertures of 43 in. or 48 in.

Reflecting Surfaces

Two kinds of vacuum-metallized plastic reflecting sur-

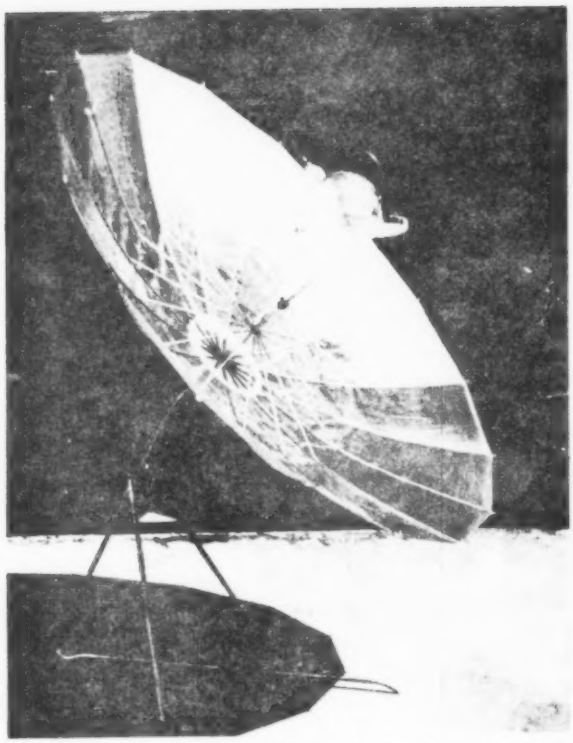

FIG. 2 — A folding reflector fabricated of a Mylar-vinyl-cloth laminate mounted on an umbrella frame, for use as a solar cooker.

FIG. 3 — The Mylar-vinyl-cloth flexible reflector, shown folded.

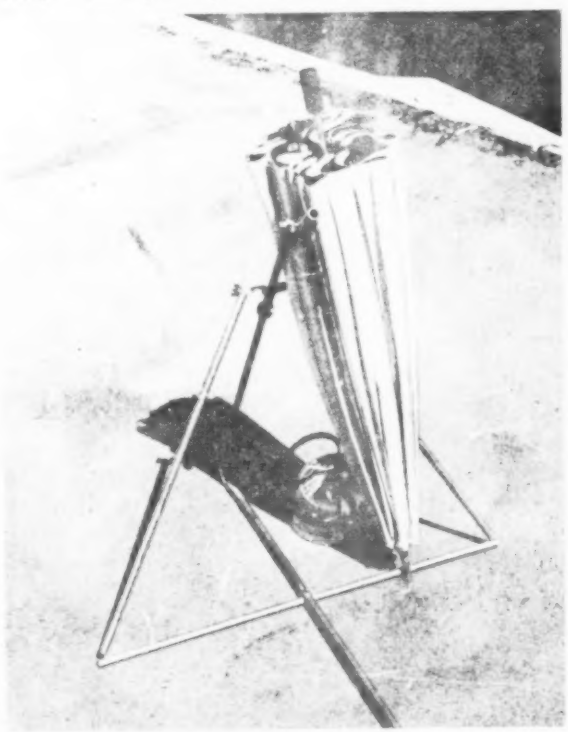

VOL.
1
1957

faces investigated in these studies were aluminized Mylar film and silvered cellulose acetate butyrate. Both of these materials can be obtained with sufficient deposited metal to provide good specular reflectivities.

The aluminized Mylar film, in the form of a pressure-sensitive tape, was applied to formed shells with the Mylar film on the outside of the aluminum layer, thus providing a protective coating over the reflective surface. The Mylar in this form was found to be convenient for application in experimental use, although costly. One-half-mil aluminized Mylar was also laminated to shell materials before drape forming, and although the higher softening temperature of the Mylar made forming more difficult, usable reflectors were obtained.

The weathering characteristics of Mylar are not completely known. Unsupported samples of the clear and aluminized film became cloudy and brittle after exposure for several months. Supported samples of aluminized Mylar are still in fairly satisfactory condition after more than 1.5 years of continuous outdoor exposure at Madison and exhibit specular reflectivities for direct solar energy of about 60 per cent, with the reduction apparently due to clouding of the film. The average specular reflectivity of a number of new samples of the aluminized film was 87 per cent, measured on the film side. Aluminized Mylar, when properly supported, appears to be a good reflecting material for a period of a year or more in the Madison climate and was used in the fabrication of all of the complete solar cookers tested. Aluminized weatherable Mylar, recently developed by du Pont, is expected to have substantially better life.

Cellulose acetate butyrate with a vacuum-deposited layer of silver was considered for a reflecting surface because of the excellent weathering characteristics of the plastic material and the ease with which it can be vacuum formed. In brief experiments, 20- and 30-mil samples of the silvered material were vacuum formed to the curvature used in the reflectors. The forming operation resulted in an average area increase of approximately 10 per cent and some reduction of reflectivity, with the silver layer apparently losing its continuity. These samples had only light coatings of silver, and the reflectivities could be improved with heavier layers. No complete cookers using this material were tested.

Fiberglass-Reinforced Polyester Shells

Fiberglass-reinforced polyester reflector shells were made by a hand-layup molding technique on the convex side of the aluminum molds, using both woven glass fiber cloth and mat. Aluminized Mylar tape was applied to these shells to provide the reflecting surface. These performed satisfactorily as experimental cooker reflectors. In the fabrication of these shells, Selectron 5003 with methyl ethyl ketone peroxide catalyst and cobalt napthenate (6 per cent cobalt) accelerator were used, with styrene monomer as a reactive diluent for viscosity reduction. Curing was accomplished at room temperature; by this method, matched dies were not required. With 2-oz glass mat, 4.5 lb polyester mix were used to form a shell approximately $\frac{1}{8}$-in. thick; with woven glass cloth, 3 lb of polyester were required. To stiffen the thinner cloth-reinforced shells, radial ribs of fiberglass cloth and polyester were formed on the back of the shells. The shell material was formed around a stiffening peripheral rim of $\frac{3}{8}$-in. aluminum tubing. These techniques required about two man-hours for fabrication of each shell.

Polystyrene Shells

Rubber-modified or high-impact polystyrene is an inexpensive, readily available material which can be easily formed by vacuum- and drape-molding techniques. It has a tendency to become cracked or crazed on exposure to ultraviolet radiation; however, with a reflective lining covering the front surface and a suitable protective coating on the back surface, a shell should have satisfactory life. This appears to be the most promising reflector shell material for solar cooker application, and it is being investigated for other applications.

Both vacuum- and drape-molding techniques were used, with each having advantages. The former, accomplished on a concave mold, results in molded pieces having minimum reduction in thickness at the outer edge; thus maximum stiffness is obtained at the reflector shell periphery, where it is most desired. Drape molding, on a convex mold, results in maximum draw and reduction in thickness at the periphery but has the advantages that laminates of the shell material to reflective material can be heated by radiation from the nonreflecting side, and radial ribs on the back sides of the shells can be formed by convex rib molds.

High impact polystyrene sheets in 40- and 50-mil thicknesses were formed into parabolic shells by standard vacuum- or drape-molding techniques. Some of the shells were formed with radial ribs which provided rigidity when thinner materials were used; Fig. 4 shows a ribbed drape-molded shell being removed from the mold. Rims of $\frac{3}{8}$-in. aluminum tubing were applied by heating the edges of the formed sheet and rolling the plastic around the rims, or by cementing with a caulking compound which adheres to both aluminum and polystyrene. The backs of the reflectors were sprayed with a commercial

FIG. 4 — A ribbed, drape-molded polystyrene reflector shell being removed from the mold.

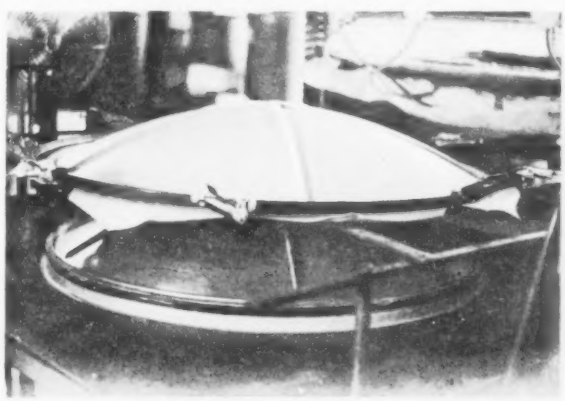

coating and aluminized Mylar pressure-sensitive tape was used as a reflective lining.

The dimensional stability at elevated temperatures of sample pieces of 50-mil formed material was checked by heating in an oven at 175° and 185°F for four hours; no measurable return to the original (flat) shape was observed at the lower temperature, but the sample of 185°F had partially flattened.

Concentration ratios of about 300 are easily obtained with both vacuum- and drape-formed polystyrene shells and with fiberglass-reinforced polyester shells. These ratios are satisfactory for solar cooker use, and although much higher values can be obtained, they are undesirable in this application.

Cellulose Acetate Butyrate Reflectors

The good weathering characteristics of cellulose acetate butyrate and the ease with which it can be formed by vacuum or drape molding led to trial of this material in 20-, 30-, and 40-mil thicknesses for reflector shell construction. Clear and silvered butyrate were both used in vacuum-forming experiments, the clear shells receiving a lining of aluminized Mylar tape. The peripheries of the formed butyrate shells were stiffened with aluminum rims as were the polystyrene shells, and radial ribs were formed in some. The resultant shells, with or without the ribs, were found to be unsatisfactory because of lack of stiffness and excessive material costs.

Flexible Plastic Reflectors

In the flexible type of solar reflector, an array of thin, flexible radial metal ribs supports the reflective surface in the required shape. A thin metallized plastic film, laminated to a serviceable and pliable fabric or plastic backing, is stretched on this framework in the general shape of an umbrella and folds in the same fashion. Parabolic form is secured by proper shaping of the dimensionally stable plastic or fabric laminate.

Aluminized Mylar polyester film has been employed as the reflective surface in flexible reflectors. Laminates of ½-mil metallized Mylar to a thin vinyl and cotton fabric combination ("Fabrilite") and to a light gauge rayon cloth have been used. The Mylar-vinyl-cotton combination has excellent strength, high specular reflectivity, and satisfactory folding and crease-resistant characteristics. The Mylar-rayon laminate is sufficiently strong and durable although lighter in weight, but the fabric weave shows slightly on the aluminized surface, causing some reduction in specular reflectivity. Both laminates have been employed in several models of portable solar cookers and are considered satisfactory.

Since the umbrella ribs will assume the curvature into which they are forced by the fabric or plastic cover, the shaping and assembly of the reflective segments dictate the contours of the reflector. Between adjacent ribs, the material is taut and hence has only simple radial curvature, being planar circumferentially. The complete reflector is therefore composed of several narrow, wedge-shaped cylindrical parabolas, separated from each other by and intersecting at the flexible ribs, and all intersecting at the center or axis of the reflector.

The construction of a fabric-backed reflector requires the cutting of individual segments according to pattern, each to fill the width from one rib to the next. These pieces are then machine-sewed together to form a complete, roughly circular assembly. This material is attached to the framwork by stitching the fabric to the rib tips at the outer end of each fabric seam.

The concentration ratio of the flexible reflector is not so high as that obtained with the rigid reflector because of the more diffused focus of the intersecting cylindrical segments. Rather than being a small circle, the solar image produced by the flexible reflector is a set of thin lines intersecting on the axis of the reflector at its true focal distance. Since the total width of the focal area is equal to the maximum segment width, substantial concentration ratios (50 or more) require the use of at least 16 ribs.

In the flexible reflector construction experiments, standard 16-rib metal umbrella frames have been used, with 18-in., 24-in., and 29-in. ribs. The respective apertures of the reflectors on these frames are 34 in., 45 in., and 54 in. Corresponding intercepting areas and approximate heat reflecting rates (assuming 70 per cent specular reflection of a direct solar flux of 5 Btu per sq ft per min) are: 6.3 sq ft and 0.26 kw; 11 sq ft and 0.66 kw; and 15.9 sq ft and 0.96 kw.

Performance and Costs of Solar Cookers

The heating rates of reflective-type solar cookers depend on factors other than the characteristics of the reflectors and the direct solar flux. Among these factors are the absorptivity of the container and the rate of heat loss from the container, particularly by evaporation. With suitably blackened and covered containers, a quart of cold water can be brought to a boil in about 15 minutes on clear days with either the 54-in. aperture folding reflector or the 43-in. aperture rigid reflectors. A net average heat delivery of about 20 Btu per min, in excess of the heat losses from the container, is thus obtained. Used as broilers, the reflectors can cook meats by direct irradiation, with hamburgers or steaks taking 10 to 20 minutes to cook on the 54-in. folding reflector. The cookers are well adapted to boiling, stewing, and frying operations, and have been used for baking with the addition of a small oven placed over the focal zone.

High-impact polystyrene extruded sheet material costs are in the range of 50 to 80 cents per lb; a 50-mil sheet weighs approximately 0.28 lb per sq ft. The cost of aluminized ½-mil Mylar is about 2½ cents per sq ft without laminating adhesive. To these material costs must be added the costs of supports, fabrication, etc. The costs of manufacturing the rigid plastic-shell reflector cookers has been estimated to be in the range of $6.00 to $10.00, depending on the details of the design. The costs of manufacturing the flexible reflector cookers has been estimated to be in the range of $7.00 to $10.00.

VOL.
1
1957

DISCUSSION

Other Materials

There are a number of other plastic materials having some desirable characteristics for reflecting surfaces or shells, and there are other techniques of reflector fabrication which have not been completely investigated. Other metallized films which would form readily, which would retain their clarity, and which could be applied as laminates to the shell material before forming are of interest. Shells could also have reflective coatings applied after forming by metallizing, by deposition of metals from solution or electro-deposition followed by application of a clear protective layer. The use of aluminum foil is attractive because of its low cost and availability with good specular reflectivity. It cannot be easily formed to compound curvatures, but it has been applied experimentally to reinforced polyester cylindrical shells and can be protected with an oxide or other coating.

Polymethyl methacrylate, low pressure polyethylene, rigid polyvinyl chloride, polyvinyl chloride-acetate copolymers, and styrene-butadiene-acrylonitrile blends are possible materials for shell fabrication which have not yet been used, either because of unavailability or high present price. Fabrication of the flexible reflectors may possibly be simplified by drape or vacuum forming of thermoplastic laminates of polyvinyl chloride-aluminized Mylar or similar combinations, followed by fastening of the formed sheet to the rib tips.

Other Applications of Plastic Reflectors

The 43-in. aperture rigid parabolic reflectors are being used experimentally in solar regeneration of small absorption refrigeration units. Aluminized Mylar has been applied to Masonite and polystyrene cylindrical shells and fiberglass-reinforced polyester cylindrical-parabolic shells, both for experimental steam generation studies. Also under study as steam generators are spherical reflectors of vacuum-formed polystyrene supported on tubular frameworks.

Conclusions

Several plastic materials show promise in the fabrication of focusing solar reflectors. The prospects for low-cost collection of solar energy merit their evaluation for several possible applications. Of the materials investigated to date, aluminized Mylar, laminated to formed, high-impact polystyrene shells, appears to be the most promising low-cost combination for fabrication of rigid reflectors. Direct-type solar cookers with these reflectors and some with fiberglass-reinforced polyester shells, designed for nonindustrialized areas, have performed acceptably in experimental use for several months. Flexible laminates of aluminized Mylar and vinyl-coated cloth have also been successfully applied in folding solar reflector cookers. The flexible reflector is more costly and less sturdy than the rigid plastic reflectors; however, its principal usefulness is considered to be where its portability is important, as in solar cookers for outdoor recreational use. Further studies are in progress on other materials, fabricating methods, and applications.

ACKNOWLEDGEMENTS

The studies herein reported on rigid reflectors and cookers were carried out as part of a program on solar energy research at the University of Wisconsin, supported by the Rockefeller Foundation, the Engineering Experiment Station of the University, and the National Science Foundation. The advice of Professor Farrington Daniels has contributed substantially to this study, and Mr. D. C. Dunham is responsible for much of the design work on the Wisconsin cooker.

REFERENCES

1. E. J. Burda (ed.), *Applied solar energy research*. Menlo Park, Calif., Stanford Research Institute, 1955.
2. F. Daniels and J. A. Duffie (eds.), *Solar energy research*. Madison, Univ. of Wisconsin Pr., 1955.

CONCENTRATION OF THE SOLAR RADIATION IN A SOLAR FURNACE

By TARO HISADA, HISAO MII, CHOJI NOGUCHI, TETSUO NOGUCHI, NOBUHEI HUKUO and MASAO MIZUNO

Government Industrial Research Institute, Nagoya, Japan

Energy concentration in a solar furnace is greatly influenced by the optical accuracy of the reflecting surface of the mirror. The highest density of a heat flux on the heating surface of a specimen is determined by its concentration and by the reflectivity of the mirror.

Since the apparent diameter of the moon is almost equal to that of the sun and the illumination of the moon may be adapted to the photographic determination of flux density, the rate of energy concentration in the authors' solar furnace was studied by the moon's image projected upon the heating zone in place of that of the sun.

As a result, about 300 watts per cm was obtained as the highest possible density of the heat flux in this solar furnace. This figure also agreed with the results of an optical analysis based on the practical finishing of the present mirror surface. With a heat flux of 300 watts per sq cm, in accordance with Stefan-Boltzmann's law of radiation, the highest temperature attainable is estimated to be approximately 2700°K. Besides the above, in actual experiment, approximately 2300°C was obtained in observing the melting points of binary mixtures, e.g., MgO-CoO and $MgO\text{-}Cr_2O_3$. Thus, the above-mentioned three approaches to the problem are in fairly good agreement.

INTRODUCTION

The total amount of energy and the density of the heat flux concentrated on the heating surface of the specimen are the two most important factors in calculating the possibilities of a solar furnace. The concentrated total energy depends upon the incident solar radiation, the aperture, and the reflectivity of the reflecting mirror, while the density of the heat flux depends upon the reflectivity and optical accuracy of the mirror, the accuracy in positioning a specimen, the sun-tracking accuracy, etc. However, the two most important factors to be considered are the reflectivity and optical accuracy of the mirror.

This paper follows our previous paper[1] on the theoretical analysis of a solar furnace In it, the characteristics

FIG. 1 — The moon's image on the heating surface of a specimen. Exposure time: (A) 1 sec; (B) 3.5 sec; (C) 6 sec.

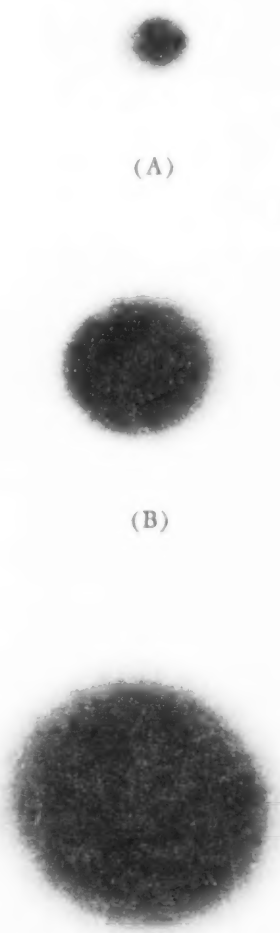

(A)

(B)

(C)

VOL. 1 1957

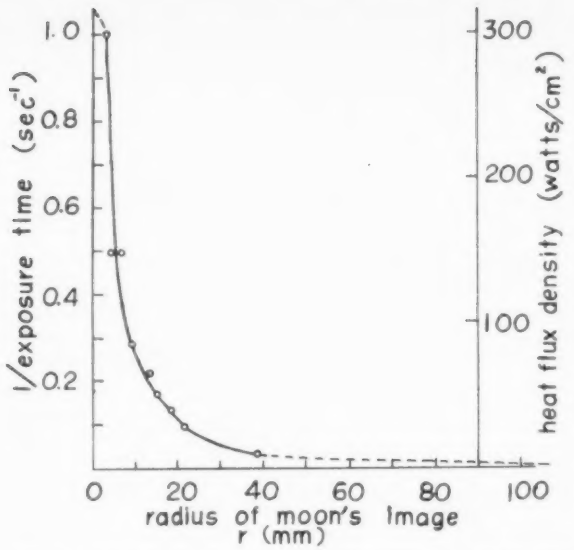

FIG. 2 — Distribution of lunar radiation concentrated on the heating surface.

of our furnace, covering the above-mentioned items, were discussed.

THE DETERMINATION OF HEAT FLUX USING LUNAR RADIATION

It is difficult to examine the density of the heat flux on the heating surface using direct solar radiation because of the very high temperatures produced. Assuming that the distribution of the surface brightness of the moon is proportional to that of the sun and since the apparent angular diameter of the moon is almost equal to that of the sun, the heat flux distribution of the furnace may be obtained by focusing the moon's image on the surface of the specimen. It is believed that this assumption is sufficiently correct that an approximate estimate of the heat flux of a solar furnace may be made.

Measurements were made on the night of a full moon. The moon's image was focused on the focal plane to which bromide paper had been affixed, and the moon was tracked. The accuracy in setting the bromide paper and in tracking the moon was kept to the same degree as when the sun is used as the source of light.

Some of the results are shown in Fig. 1, where the exposed patterns, i.e., exposed images, form approximately concentric circles whose diameters increase with an increase in the exposure time.

The brightness of the moon's image at the periphery of each pattern is assumed to be proportional to the reciprocal of the exposure time. Fig. 2 shows the relationship between the radius of the exposed image and the reciprocal of the exposure time. The left-side ordinate of Fig. 2 may be thought of as the brightness of the moon's image, i.e., the density of the heat flux by solar radiation; then the ordinate of the density, E watts per sq cm, shown at the right side of Fig. 2, may be calculated by the following procedure:

Provided that Fig. 2 indicates the heat flux of solar radiation, the total energy concentrated on the heating zone is equal, in watts per sq cm, to

$$\pi \int r^2 dE \qquad [1]$$

This amount must also be equivalent to the value when the effective area of the mirror is multiplied by the reflectivity and by the direct solar radiation. Since the aperture and reflectivity of our furnace are 2 m and 0.5 $\sim$ 0.6, respectively, the following equation must be true

$$\pi \int r^2 dE \approx 0.55\pi \times 10^3 \qquad [2]$$

where the direct solar radiation at the furnace site is assumed to be 0.1 watts per sq cm. The integration is performed by means of a planimeter from Fig. 2, and the result is shown as the ordinate at the right side in Fig. 2. The most intensive flux is thus estimated to be about 300 watts per sq cm.

EFFECTS OF THE OPTICAL ACCURACY OF THE MIRROR SURFACE

This section discusses agreement between the above result and that estimated from the optical accuracy of the present mirror surface. The method of machining and finishing the present mirror surface is as follows:

Fig. 3 shows the principle of parabolizing the reflector. Let us say that the intersections of the optical axis and the normals of the paraboloid at P and Q are O_1 and O_2, respectively, and the intersection of the two arcs whose radii are O_1P and O_2Q is R. Then the paraboloid may be formed by joining the arcs PR, RQ, etc., where the interval O_1O_2 is fixed at 5 mm. In practice, cutting the mirror in accordance with this principle of parabolizing is difficult to accomplish on an ordinary lathe, because it is difficult to maintain the necessary accuracy during the rotation of the cutter arms corresponding to O_1P, O_2Q, etc., to form the arcs PR, RQ, etc. Thus a rotating cutter

FIG. 3 — Principle of parabolizing.

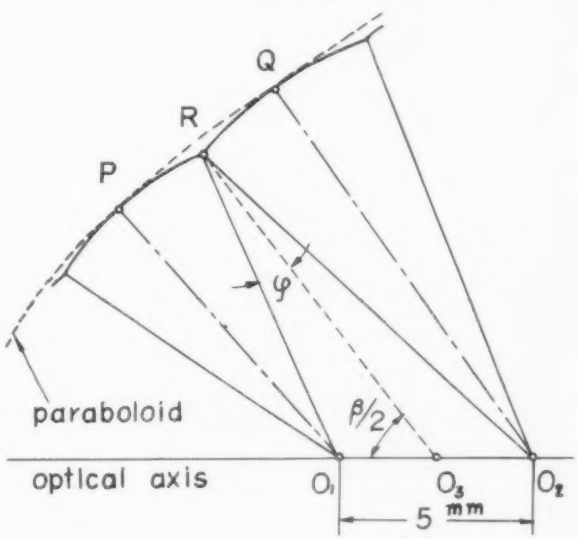

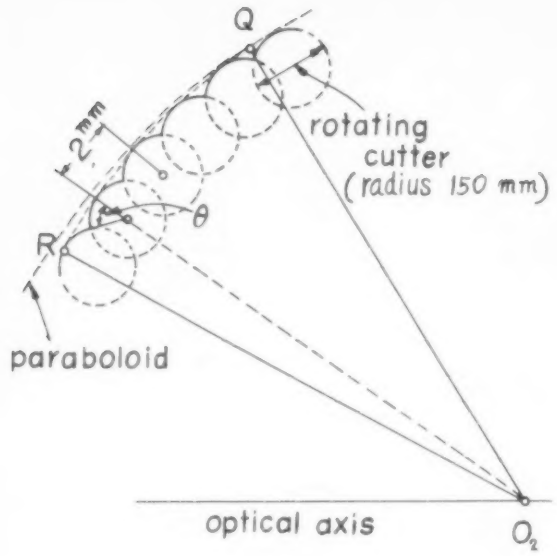

FIG. 4 — Method of cutting the reflector.

having a radius of 150 mm was attached to the arm, and, for example, the arm O_2Q was rotated to form the arcs with 2 mm pitch as shown in Fig. 4. After the cutting work was completed, the surface of the mirror was polished by hand with charcoal to remove the trace of waviness. Then the mirror was buff-finished, with a rotating felt-buff exchanged for the above rotating cutter.

The accuracy of the reflecting surface may be determined by the size of the angle formed by the normals of the ideal paraboloid and those of the reflecting surface actually achieved. For example, when the angle as shown in Fig. 5 is assumed to be ϕ, the reflected ray will be inclined with the angle 2ϕ from the reflected ray of the ideal paraboloid. The angle in Fig. 3 is maximum at R. Provided that the normal of the ideal paraboloid passing through R is RO_3, the angle in Fig. 3 may be represented as ϕ.

In Fig. 5, the length of RO_3 is equal to $\sqrt{4f(f+x)}$ or $2f\sqrt{2/(1+\cos\beta)}$, where f is the focal length and β is the angle RFO. Since it can be assumed that the length O_1O_3 is approximately equal to 2.5 mm, the approximate value of ϕ in Fig. 3 may be obtained by applying the sine formula for triangle RO_1O_3 as follows,

$$\phi \approx (1.25/f)\tan(\beta/2) \qquad [3]$$

In our furnace,

$$f = 640 \text{ mm},\ \beta = 0 \sim 76^\circ \qquad [4]$$

then

$$\phi \approx 0 \sim 0.002 \times 0.77 = 0 \sim 0.0016 \qquad [5]$$

In Fig. 4, the angle formed by the normal of the arc RQ and that of the cutting surface is equal to $0 \sim \theta$, where θ is an angle as shown in this figure. θ may be approximated by the equation

$$\tan\theta = 1/150 \qquad [6]$$

Then

$$\theta \approx 0.0067 \qquad [7]$$

Thus the size of the angle formed by the normal of the ideal paraboloid and that of the cutting surface in Fig. 4 is indicated as the sum of Equations [5] and [7], i.e.,

$$0 \sim 0.008(3) \qquad [8]$$

When the parabolic reflector is finished within the above error, the reflected ray will deviate from that of the ideal paraboloid by twice the angle in Equation [8]; i.e.,

$$0 \sim 0.016 \qquad [9]$$

Since the apparent angular radius of the sun is equal to 0.0046, the ratio of the above deviation range, the scattering range of the focal point, to the solar image by paraxial ray becomes

$$0.016/0.0046 \approx 3.4 \qquad [10]$$

Since it is thought that the probability of scattering in this range is everywhere uniform, the value in Equation [10] will be regarded as the value of b/d mentioned in our previous paper.[1] In Equation [10] the effect of hand-finishing is not considered; however, if it is taken into account, the value in Equation [10] of the present reflector will have to be smaller. Some inspections carried out after the last buffing have shown it to be in the neighborhood of 2.0 ~ 2.5.

The maximum density of the heat flux in our furnace, under the condition that the direct solar radiation is equal to 0.1 watts per sq cm, may be described by Equation [4] of our previous paper:[1]

$$E_m = (4 \times 0.55 \times 0.1 \times 0.97^2/0.93^2) \times 10^4 = 2390 \text{ watts/cm}^2 \qquad [11]$$

If the aperture ratio is equal to 2.3 and b/d is equal to 2.5, the maximum density of the heat flux may be obtained by multiplying 0.2 by Equation [11] in accordance with

FIG. 5 — Scattering caused by optical error in the mirror surface.

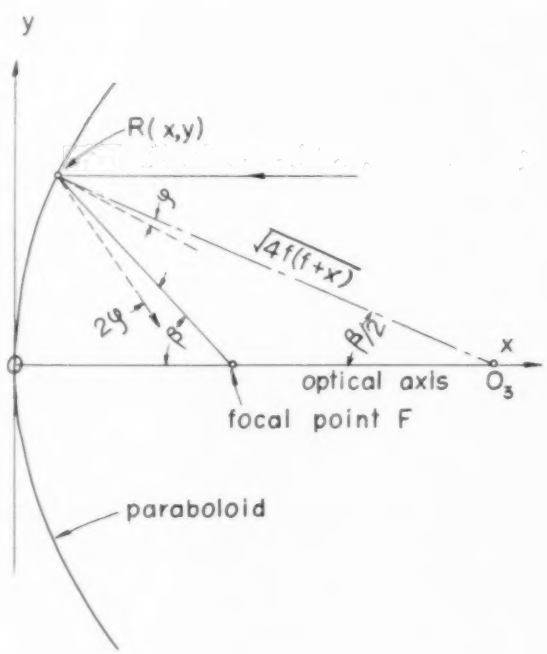

VOL.
1
1957

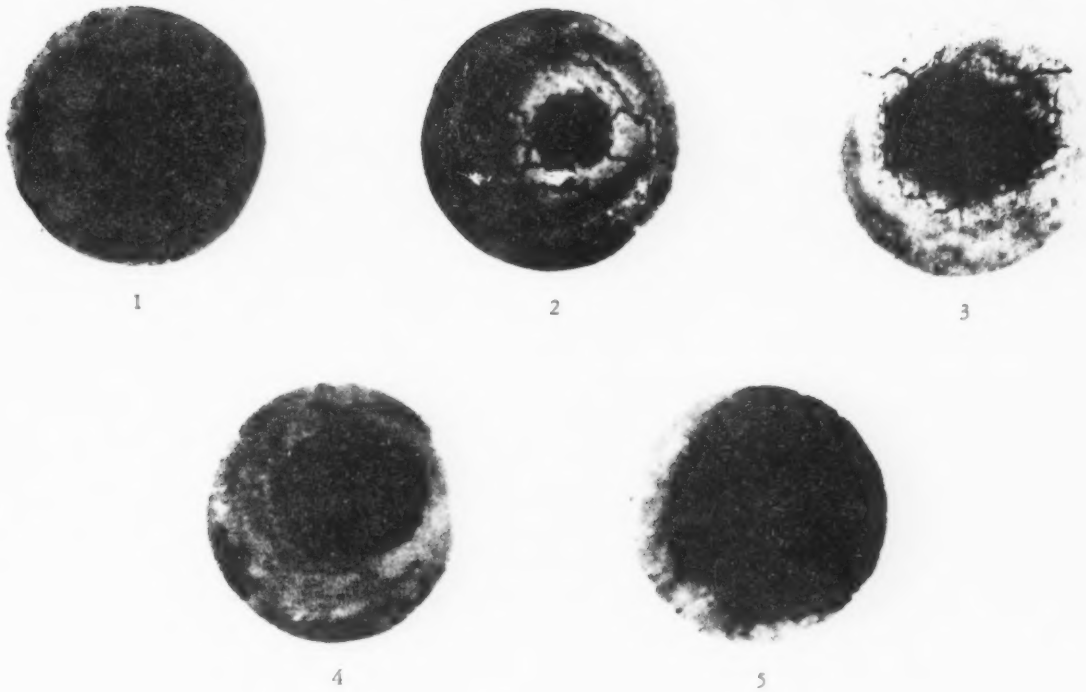

FIG. 7 — Heated samples of MgO-CoO system.

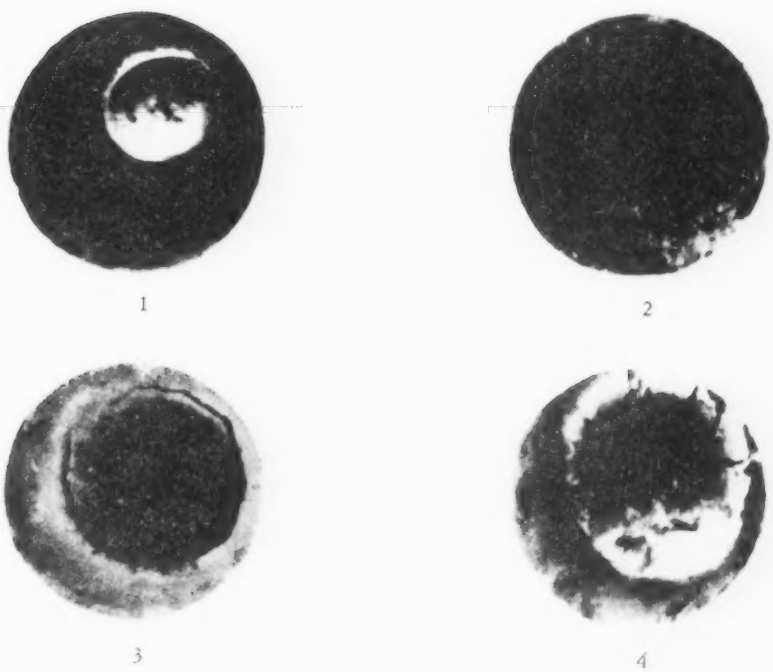

FIG. 8 — Heated samples of MgO-Cr_2O_3 system.

VOL.
1
1957

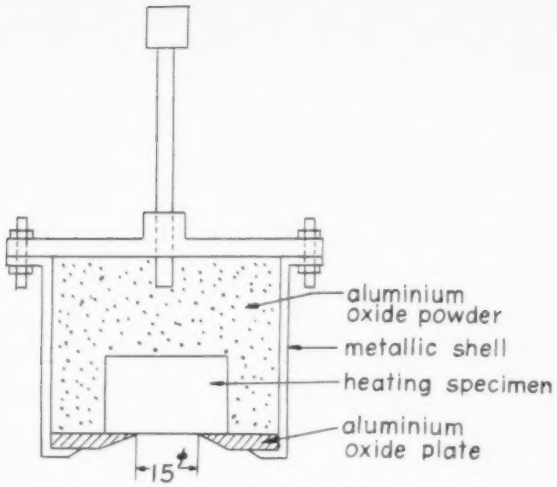

FIG. 6 — Sample holder.

the result in Fig. 14 of the previous paper.[1] Since the aperture ratio of our parabolic reflector is 3.12, the multiplying factor 0.2 becomes smaller, i.e., about 0.12 ~ 0.15; therefore, the predictable value of the flux density may be obtained by the following: 2390 × (0.12 ~ 0.15) = 285 ~ 360 watts per sq cm. Thus the maximum heat flux density of 300 watts per sq cm estimated from the moon's image reflected by the present mirror surface is in agreement with the above result calculated from the viewpoint of optical accuracy.

ATTAINABLE TEMPERATURE

In actually heating a specimen in the solar furnace, it is desirable for the specimen to approach a black-body condition; however, several metal oxides having a high melting point are apt to show relatively small absorptive power and reflect most of the solar radiation coming from the reflector. For example, pure silica, alumina, etc., were observed to be rather difficult to melt because of their white colour, i.e., poor absorptivity even though a conical cavity was prepared on the heating surface of these specimens. A sample holder was then designed as shown in Fig. 6 to reduce the heat losses.

Specimens of 30 mm were molded under a pressure of 300 kg per sq cm and held on the aluminum oxide plate by filling up the excess space in the holder with alumina powder.

To measure the temperature practically attainable in our furnace, varying binary combinations of MgO-CoO and MgO-Cr_2O_3 were melted and observed (see Table I). The results are shown in Figs. 7 and 8. The average intensity of direct solar radiation during the operation was 0.9 cal per sq cm per min, melting being observed on the heating surface of the specimens within a few seconds.

As shown, melting occurred throughout the entire MgO-Cr_2O_3 system, and in No. 1 and No. 2 of the MgO-CoO system. In No. 3 and No. 4 of the latter system, the samples were only partially sintered, and the No. 5 sample

TABLE I.
COMBINATIONS OF THE BINARY MIXTURES
(MOLAR PER CENT)

Sample No.	1	2	3	4	5
MgO	0	20	50	80	100
CoO	100	80	50	20	0

Sample No.	1	2	3	4	5
MgO	0	20	40	60	80
Cr_2O_3	100	80	60	40	20

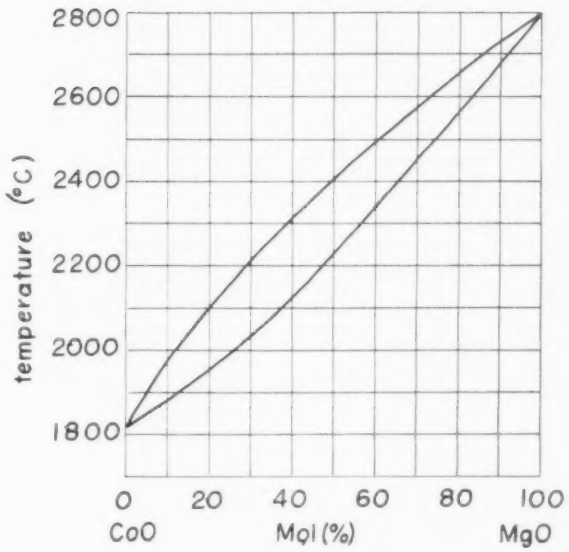

FIG. 9 — Phase diagram of the MgO-CoO system.

FIG. 10 — Phase diagram of the MgO-Cr_2O_3 system.

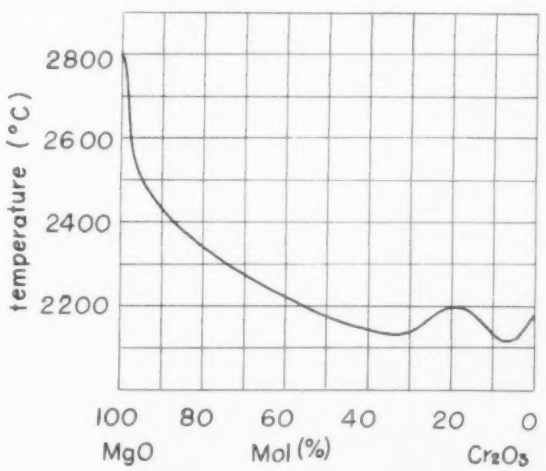

of pure white MgO was neither melted nor sintered, but remained untouched by the heat.

Collating the above results to their phase diagrams as shown in Fig. 9 and Fig. 10,[2] the maximum temperature attainable was estimated to be approximately 2300°C.

When Stefan-Boltzmann's law of radiation is applied to the solar furnace, the maximum temperature attainable may be calculated as 2700°K using the maximum heat flux density of 300 watts per sq cm as obtained above. The aforementioned calculations show rather good agreement between the maximum heat flux density of our solar furnace and the highest temperature attainable as calculated using Stefan-Boltzmann's law of radiation.

SUMMARY

The results for the concentration of solar radiation in our furnace are in agreement using three separate methods of calculation, namely, the estimation of the concentration by the moon's image, by optical accuracy of the mirror surface, and by practical heating tests of some binary mixtures. It may be concluded that the maximum heat flux density is about 300 watts per sq cm and that the maximum temperature practically attainable is approximately 2300°C. To obtain greater concentration of solar rays and higher temperatures, a more accurate mirror surface and higher reflectivity of the reflector must be achieved.

REFERENCES

1. Nobuhei Hukuo and Hisao Mii, "Design problems of a solar furnace." *J. Solar Energy Sci. Eng.* 1(2-3): 108-14, Apr.-July 1957.
2. E. M. Levin, H. F. McMurdie and F. P. Hall, *Phase diagrams for ceramists.* 1956. p. 50, 55.

VOL.
1
1957

THE FLUX THROUGH THE FOCAL SPOT OF A SOLAR FURNACE*

By PAUL D. JOSE

Holloman Air Development Center, Alamogordo, N.M.

An analysis is made of the flux through the focal spot of a solar furnace, taking into account the limb darkening of the sun.

The intensity of the apparent disk of the sun is not uniform. It is greatest at the center and falls off toward the limb. In any image-forming device this gradation of intensity will be reflected in the image. A camera, for which the focal ratio is reasonable, will exactly duplicate the intensity distribution in the image. However, a solar furnace has a focal ratio of the order of 0.5, or, in furnace language, an aperture ratio of 2. This large aperture ratio produces a spread in the image and complicates the problem of computing the flux.

The relative intensities at different radial distances from the sun's center are given in Table I.[1]

TABLE I

RELATIVE INTENSITY ALONG A RADIUS OF THE SOLAR DISK

r	I
.00	100.0
.50	93.4
.75	78.8
.98	49.0
1.00	39.0

An empirical equation[2] which fits the data to a fair degree is

$$I = \frac{1 + 1.5641 \cos \beta}{2.5641} I_o \qquad [1]$$

where I_o is the intensity at the sun's center and β is the angle at the center of the sun which subtends a radius r on the apparent solar disk.

In Figs. 1a and 1b, R_o is the radius of the apparent solar disk. The value of R_o depends on the size of the image. Since $\cos \beta = \sqrt{R_o^2 - r^2}/R_o$ Equation [1] may be written

$$I = \frac{R_o + 1.5641 \sqrt{R_o^2 - r^2}}{2.5641 R_o} I_o \qquad [2]$$

The value of I_o may be determined as a function of R_o and the solar constant, 1.94 cal per sq cm per min. The calculations are based on 100 per cent efficiency and conditions above the earth's atmosphere. R_o is the radius of the image of the solar disk formed on a plane which is perpendicular to the axis of the cone of light reflected from a projected area of 1 sq cm on the parabolic condenser. The power passing through this circular image is therefore 1.94 cal per min. We have then

$$E = 1.94 \text{ cal/min} = \int_o^{R_o} I \, ds = 2\pi \int_o^{R_o} Ir \, dr \qquad [3]$$

where (Fig. 1a) $ds = 2\pi \, rdr$ is the increment of area of a concentric circular zone. Inserting the value of I from Equation [2] into Equation [3] and integrating we have

$$I_o = \frac{0.77513}{R_o^2} \qquad [4]$$

Equation [2] becomes

$$I = \frac{1}{R_o^3}\left[qR_o + t\sqrt{R_o^2 + r^2}\right] \qquad [5]$$

$$q = 0.30230 \qquad t = 0.47283$$

Equation [5] gives the intensity at any point along a radius of the image of the sun which is formed by the light reflected from an area which projects into 1 sq cm perpendicular to the directions of the incident sunlight.

If the apparent disk of the sun were of uniform intensity, we would have

$$E_f = 1.94 = I_f \int_o^{R_o} ds = \pi I_f R_o^2 \qquad [6]$$

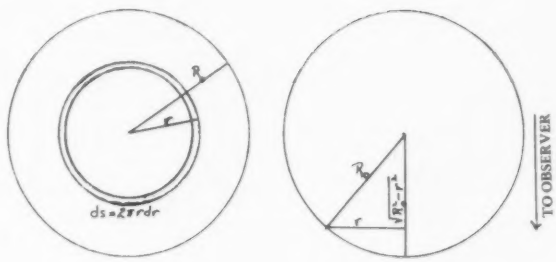

FIG. 1-a — The apparent solar disk.
FIG. 1-b — Definition of θ.

*A condensation of Technical Memorandum HDRRM-TM-57-3, Holloman Air Force Base.

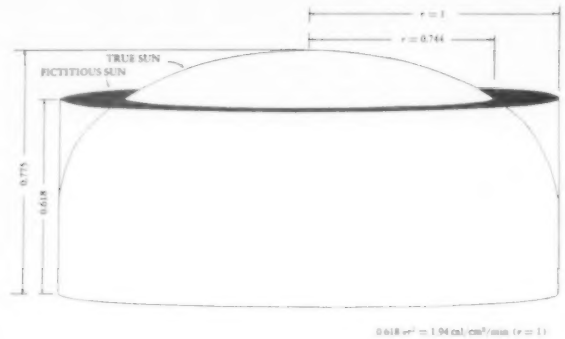

FIG. 2 — Power distribution in the surface of the true sun compared to the fictitious sun.

$$I_f = \frac{0.61752}{R_o^2}$$

Fig. 2 illustrates the power output of the two suns, where R_o is taken as unity. Their intensities are the same at $r = 0.744R_o$.

The focal spot of a solar furnace is considered to be the circular area in the focal plane which is produced by the sunlight which is reflected from the vertex of the parabolic condenser. The radius of this spot is $R_a = Fa/2$, where F is the focal length and a is the apparent angular diameter of the sun. The cone of light which is reflected from any point of zone angle θ has a circular cross section of radius

$$R_o = \frac{\rho a}{2} = \left(\frac{2F}{1+\cos\theta}\right)\left(\frac{a}{2}\right) = \frac{2R_a}{1+\cos\theta} \qquad [7]$$

In the vicinity of the focal plane, the reflected cone of sunlight is considered to be a right circular cylinder of radius R_o. The flux through an elliptical area centered on the circular cross section of the cylinder (Fig. 3) is the part of the total flux which passes through the circular focal area. Fig. 4 represents the cross section of the cylinder. The semi-major axes of the ellipse are respectively $a = R_a$ and $b = R_a \cos\theta$. The standard equation of the ellipse is $b^2x^2 + a^2y^2 = a^2b^2$.

FIG. 3 — Cylindrical approximation.

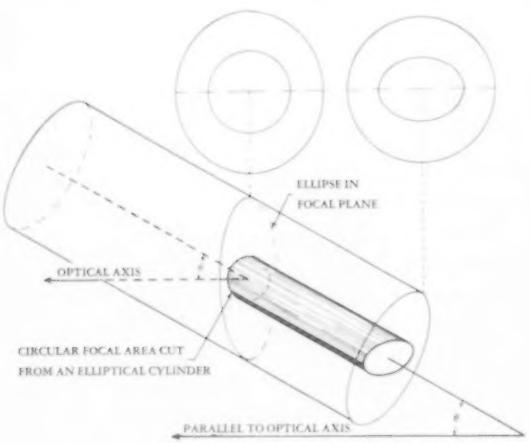

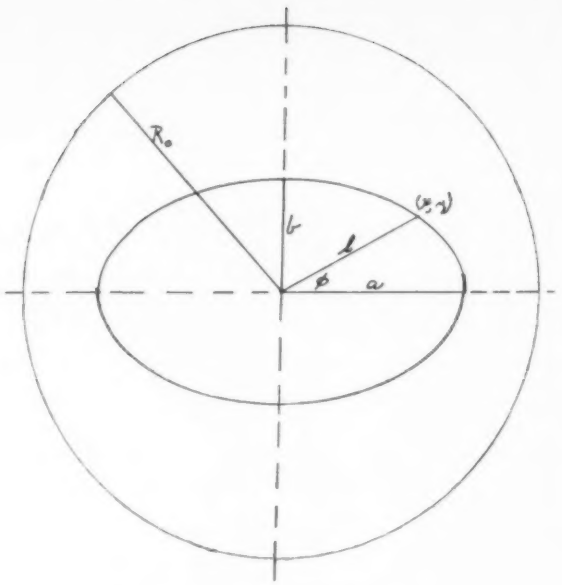

FIG. 4 — The elliptical section.

In Fig. 4 the coordinates x and y may be expressed in terms of the variables l and ϕ, where l is the polar distance and ϕ the polar angle of any point on the ellipse.

$$x = l\cos\phi \qquad y = l\sin\phi$$

and the equation of the ellipse becomes

$$l^2 = \frac{R_a^2\cos^2\theta}{\cos^2\theta\cos^2\phi + \sin^2\phi} \qquad [8]$$

The flux through any concentric area of the focal spot may be computed by letting $a = nR_a$ and $b = nR_a\cos\theta$, where $0 \leqq n \leqq 1$. The equation of the reduced ellipse is then

$$l^2 = \frac{n^2R_a^2\cos^2\theta}{\cos^2\theta\cos^2\phi + \sin^2\phi} \qquad [9]$$

The flux through the reduced ellipse is given by

$$E_n = 4\int_{\phi=0}^{\phi=\pi/2}\int_{r=0}^{r=l} Ir\,dr\,d\phi = \qquad [10]$$

$$\frac{4}{R_o^3}\int\int\left[qR_o + t\sqrt{R_o^2 - r^2}\right] r\,dr\,d\phi$$

Integration gives the expression

$$E_n = \frac{\pi q n^2\,(1+\cos\theta)^2\cos\theta}{4} + \frac{2\pi t}{3} - \frac{t(1+\cos\theta)^3n^3}{6}\times$$

$$\times\int_0^{\pi/2}\left(\frac{4}{n^2\,(1+\cos\theta)^2} - \frac{\cos^2\theta}{\cos^2\theta\cos^2\phi + \sin^2\phi}\right)^{3/2} d\phi \qquad [11]$$

The integral in Equation [11] was evaluated by quadratures for values of $n = .1, .2, \cdots 1.0$ and values of θ at every 2.5 degrees from $\theta = 0°$ to $\theta = 75°$.

E_n is the power through the central area of the focal spot of radius nR_a which is reflected from a unit projected area of the condenser.

Let ΔS be the area of a zonal ring of the parabolic condenser.

VOL.
1
1957

$$\Delta S = 2\pi\rho^2 \sin\theta \sec\frac{\theta}{2}\Delta\theta$$

$$\rho = \frac{2F}{1+\cos\theta} \qquad [12]$$

so that

$$\Delta S = \frac{8\pi F^2 \sin\theta \sec(\theta/2)\,\Delta\theta}{(1+\cos\theta)^2} \qquad [13]$$

The projected area of this zonal ring of the parabola is $\Delta S \cos(\theta/2)$. The increment of power through this ring which contributes to the focal image of radius nR_a is

$$\Delta P_n = E_n \Delta S \cos\frac{\theta}{2} = 8\pi F^2 \frac{E_n \sin\theta\Delta\theta}{(1+\cos\theta)^2} \qquad [14]$$

The total power through the focal image of radius nR_a which is reflected by all the condenser within zone θ is

$$P_n = 8\pi F^2 \int_o^\theta \frac{E_n \sin\theta}{(1+\cos\theta)^2}\,d\theta \qquad [15]$$

For each value of n ($n = .1, .2, \cdots 1.0$) the value of the integrand in Equation [15] was determined for values of θ at 2.5° intervals from $\theta = 0°$ to $\theta = 75°$. Using the Method of Least Squares Curve Fitting by Orthogonal Polynomials the data for each value of n was fitted to a polynomial of the form $\Sigma a_i\theta^i$

$$P_n = 8\pi F^2 \int_o^\theta \frac{E_n \sin\theta}{(1+\cos\theta)^2}\,d\theta \qquad [16]$$

$$= \frac{8\pi^2F^2}{180}\int_o^\theta \sum a_i\theta^i\,d\theta = \frac{8\pi^2F^2}{180}\left(\sum b_i\theta^i\right)$$

where θ in the last two expressions of the equations is in degrees. The coefficients b_i are tabulated in Table II.

The power through a concentric ring at the focal spot is

$$P_n - P_{n-0.1} = 8\pi F^2\left[\frac{\pi}{180}\left(\sum_n b_i\theta^i - \sum_{n-0.1} b_i\theta^i\right)\right] \qquad [17]$$

The area of the concentric ring between $r = nR_a$ and $r = (n-0.1)R_a$ is

$$A_n - A_{n-0.1} = \frac{\pi F^2 a^2}{4}\left[0.2n - 0.01\right] \qquad [18]$$

The power per unit area at radius $r = (n - 1/20)R_a$ is then;

$$\text{Power (cal/cm}^2\text{/min)} = \frac{P_n - P_{n-0.1}}{A_n - A_{n-0.1}} \qquad [19]$$

It is desirable to have the power in terms of seconds, hence:

$$\text{Power (cal/cm}^2\text{/min)} = \frac{1}{60}\left[\frac{P_n - P_{n-0.1}}{A_n - A_{n-0.1}}\right]$$

$$= \frac{32}{60a^2}\left[\frac{\frac{\pi}{180}\left(\sum_n b_i\theta^i - \sum_{n-0.1} b_i\theta^i\right)}{0.2n - 0.01}\right] \qquad [20]$$

Table III tabulates the rim angle θ, the fractional part of the radius of the focal spot, n; the value of $b_i\theta^i$ for each value of n; the numerator of the quantity in brackets in Equation [20] and the flux density at radius $r = (n - 1/20)R_a$. The data is illustrated in Fig. 5.

Fig. 6 illustrates in a different manner the data of Table III. The dotted lines in Figs. 5 and 6 represent the flux density on the assumption that the sun's image is of uniform intensity.

This discussion demonstrates that the distribution of power across the sun's disk is important in determining the performance of a solar furnace. It should be remembered that the above results are based on 100 per cent performance.

TABLE II

COEFFICIENTS $\int \Sigma\, a_i\,\theta^i\,d\theta = b_1\theta + b_2\theta^2 + \ldots b_7\theta^7 + b_8\theta^8$

n	b_1	b_2	b_3	b_4
.1	-1.100×10^{-6}	$+5.311521 \times 10^{-5}$	-5.86458×10^{-9}	$-5.1291098 \times 10^{-9}$
.2	-1.757×10^{-7}	$+2.1129653 \times 10^{-4}$	-1.245905×10^{-8}	$-2.0483566 \times 10^{-8}$
.3	-5.767×10^{-7}	$+4.7171809 \times 10^{-4}$	-3.559729×10^{-8}	$-4.4574804 \times 10^{-8}$
.4	-1.394×10^{-6}	$+8.2955046 \times 10^{-4}$	-1.136523×10^{-7}	$-7.4252514 \times 10^{-8}$
.5	-2.8260×10^{-6}	$+1.2769865 \times 10^{-3}$	-2.437305×10^{-7}	$-1.0689643 \times 10^{-7}$
.6	-6.7242×10^{-6}	$+1.8045318 \times 10^{-3}$	-5.676540×10^{-7}	$-1.3255893 \times 10^{-7}$
.7	-8.9667×10^{-7}	$+2.3897151 \times 10^{-3}$	-1.200302×10^{-7}	$-1.9934541 \times 10^{-7}$
.8	-1.8685×10^{-6}	$+3.0216550 \times 10^{-3}$	-2.845509×10^{-7}	$-2.1967923 \times 10^{-7}$
.9	-4.0224×10^{-6}	$+3.6638819 \times 10^{-3}$	-7.008857×10^{-7}	$-1.9242837 \times 10^{-7}$
1.0	-2.8619×10^{-6}	$+4.2351292 \times 10^{-3}$	-4.590732×10^{-7}	$-6.8116538 \times 10^{-8}$

n	b_5	b_6	b_7	b_8
.1	$-6.320258 \times 10^{-12}$	$+3.195129 \times 10^{-13}$	$-9.957376 \times 10^{-16}$	—
.2	$-2.464302 \times 10^{-11}$	$+1.2560845 \times 10^{-12}$	$-3.871890 \times 10^{-15}$	—
.3	$-7.200305 \times 10^{-11}$	$+2.8652148 \times 10^{-12}$	$-8.573856 \times 10^{-15}$	—
.4	$-1.902303 \times 10^{-10}$	$+5.3652810 \times 10^{-12}$	$-1.547741 \times 10^{-14}$	—
.5	$-4.058996 \times 10^{-10}$	$+8.7699760 \times 10^{-12}$	$-2.404534 \times 10^{-14}$	—
.6	$-8.831853 \times 10^{-10}$	$+1.4314658 \times 10^{-11}$	$-3.798754 \times 10^{-14}$	—
.7	$-1.307511 \times 10^{-10}$	$-2.2077330 \times 10^{-12}$	$+1.389452 \times 10^{-13}$	$-6.3350247 \times 10^{-16}$
.8	$-5.143943 \times 10^{-10}$	$-5.9119198 \times 10^{-12}$	$+2.360865 \times 10^{-13}$	$-1.0392452 \times 10^{-15}$
.9	-1.842293×10^{-9}	$-3.4113114 \times 10^{-12}$	$+3.264710 \times 10^{-13}$	$-1.4965511 \times 10^{-15}$
1.0	-5.966719×10^{-9}	$+3.3531127 \times 10^{-11}$	$+1.974324 \times 10^{-13}$	$-1.3578550 \times 10^{-16}$

TABLE III

POWER AS A FUNCTION OF RADIUS

θ	n	$\sum_n b_i \theta^i$	$\frac{Pn - P_{n-1}}{8\pi F^2}$	cal/cm²/sec at $r = (n - 1/20)\ R_s$
15°	.1	.011654	.00020339	121
	.2	.046455	.00060740	121
	.3	.103728	.00099960	119
	.4	.182399	.00137308	117
	.5	.280833	.00171799	114
	.6	.396778	.00202362	110
	.7	.527073	.00227408	104
	.8	.667342	.00244816	97
	.9	.810820	.00250416	88
	1.0	.943745	.00231997	73
30°	.1	.043515	.00075948	452
	.2	.173466	.00226806	450
	.3	.387614	.00373759	445
	.4	.682291	.00514308	438
	.5	1.052040	.00645335	427
	.6	1.489321	.00763198	413
	.7	1.983842	.00863103	395
	.8	2.521482	.00938358	373
	.9	3.081495	.00977406	342
	1.0	3.626841	.00951809	298
45°	.1	.087057	.00151943	905
	.2	.347173	.00453988	901
	.3	.776476	.00749275	892
	.4	1.368604	.01033458	879
	.5	2.114158	.01301238	861
	.6	3.000271	.01546559	837
	.7	4.009562	.01761545	807
	.8	5.118747	.01935893	768
	.9	6.294781	.02052566	719
	1.0	7.483204	.02074190	650
60°	.1	.130614	.00227964	1358
	.2	.521101	.00681529	1353
	.3	1.166461	.01126365	1342
	.4	2.058509	.01556918	1324
	.5	3.185191	.01966431	1301
	.6	4.530093	.02347297	1271
	.7	6.071355	.02690009	1232
	.8	7.779858	.02981901	1184
	.9	9.615292	.03203436	1122
	1.0	11.513668	.03313292	1038
75°	.1	.162505	.00283625	1689
	.2	.648554	.00848315	1684
	.3	1.452612	.01403346	1671
	.4	2.565655	.01942627	1653
	.5	3.974426	.02458769	1627
	.6	5.661050	.02943714	1594
	.7	7.601298	.03386372	1551
	.8	9.763915	.03774478	1498
	.9	12.105428	.04086712	1432
	1.0	14.557998	.04280542	1342

ACKNOWLEDGEMENTS

The writer is indebted to Charles Bodwell for guidance and assistance on the curve fitting techniques, and to James D. Patterson for doing the necessary work on the digital computers.

REFERENCES

1. Abetti, Giorgio, *The sun.* D. Van Nostrand Co., 1938. p. 316.
2. Minneart, M. (In: *The sun,* ed. by Kuiper. Univ. of Chicago Pr., 1953. p. 99.)

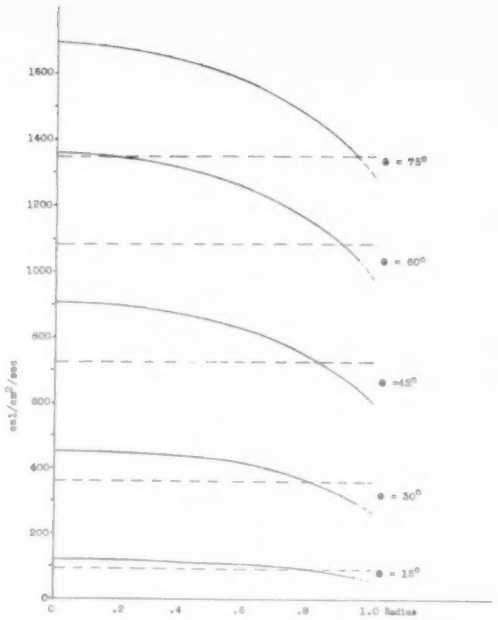

FIG. 5 — Power distribution along the radius of the focal spot for values of $\theta = 15°, 30°, 45°, 60°, 75°$.

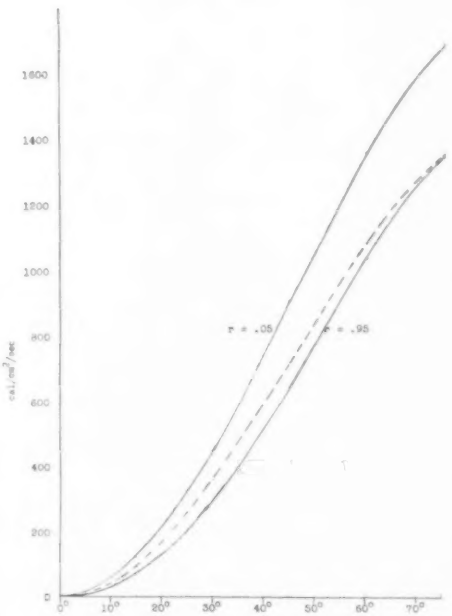

FIG. 6 — Flux density at radii 0.05 and 0.95 of focal spot as a function of rim angle. The dashed line is flux density for a "uniform" sun.

VOL.
1
1957

HEAT FLUX MEASUREMENTS AT THE SUN IMAGE OF THE CALIFORNIA INSTITUTE OF TECHNOLOGY LENS-TYPE SOLAR FURNACE*

By EUGENE LOH**, NEVIN K. HIESTER, and THOMAS E. TIETZ

Stanford Research Institute, Menlo Park, California

Flux profiles of the sun image were measured at the focus of the California Institute of Technology lens-type solar furnace using NRDL water-cooled radiometers. A maximum flux value of 220 cal per sec per sq cm was recorded when the direct solar radiation received at the furnace site was 1.04 cal per min per sq cm. Under these conditions, the furnace operating efficiency was found to be 47.2 per cent. The losses of 52.8 per cent are ascribed to transmission losses in the lenses, reflectivity losses at the mirrors, the geometrical imperfection of the individual lenses and mirrors, and lack of perfect superposition of the nineteen sets of images.

INTRODUCTION

The use of a solar furnace to obtain high temperatures has become of considerable interest recently, because of its advantages of heating in a controlled atmosphere, cavity-heating by radiation, high heat flux, and absence of large electric or magnetic fields. The Institute has recently been studying the application of such furnaces for research on solids at elevated temperatures. The work was divided into three specific areas: (a) theoretical study (1); (b) design study and cost estimate (2); and (c) experimental study (3). A portion of the latter program is the basis for this paper.

The furnace used was the lens-type solar concentrator located at the California Institute of Technology (CIT), at Pasadena. Its capabilities were determined by measuring the amount of solar energy available at the site, the amount of flux attainable at the focus, and, from them, the performance efficiency of the furnace.

In this furnace, shown in Fig. 1, lenses 2 ft in diameter with their axes pointed toward the sun collect the energy over a total area of approximately 57 sq ft. These lenses

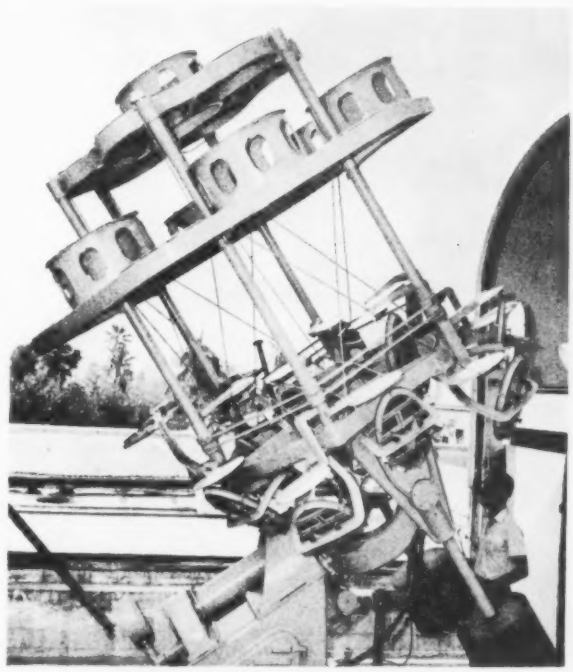

FIG. 1 — Side view of furnace.

are arranged in a hexagonal, close-packed array, with one lens in the center, surrounded by six, and then twelve surrounding the central seven. Since all the images are to be superimposed, it is necessary to arrange a series of nineteen secondary lenses on a hemisphere centered at the focal point. The sun's converging rays are then brought to these lenses by eighteen oblique mirrors. The rays collected by the central lens do not have to be deflected and so do not require a mirror. Fig. 2 partially shows this optical arrangement.

The size of the sun's image in the focal plane, i.e., the equatorial plane of the hemisphere, is 0.5 in. in diameter. The furnace is mounted like an astronomical telescope, with rotation around the earth axis and a declination axis. The focal point of the furnace is at the intersection of

*This paper is published by permission of the Air Force Office of Scientific Research of the Air Research and Development Command, under Contract AF18(600)-1499. It is based on portions of ASTIA Document No. AD110383 (AFOSR-TN-56-587), Sept. 14, 1956.

**Presently with Consolidated Engineering Corporation, Pasadena, California.

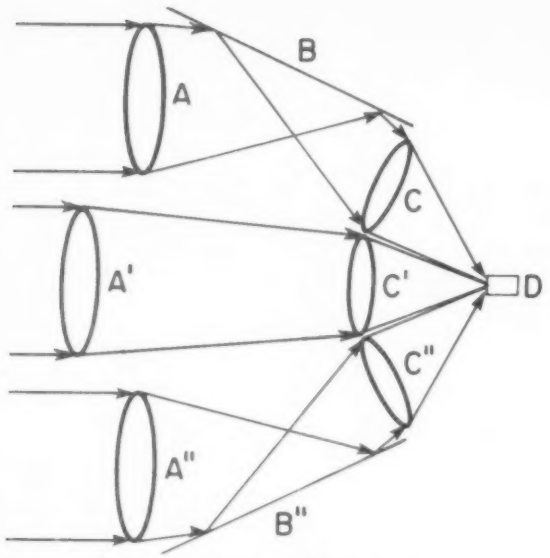

FIG. 2 — General optical arrangement.

these two axes, so that it remains fixed with respect to the ground when the furnace is tracking the sun. This tracking is achieved through a conventional astronomical drive and is automatic once the furnace has been pointed at the sun manually.

PROCEDURE

The instruments used to measure the heat flux in these experiments were two radiometers obtained from the Naval Radiological Defense Laboratories, San Francisco. These radiometers consist of a 0.0028-in.-thick silver foil disk, spot-welded over a 0.100-in. hole passing through a copper cylinder. The silver foil is blackened with platinum-black over the 0.100-in. area. As the disk receives heat flux, the absorbed heat flows from the silver foil to the copper block, which is maintained at a constant temperature by cooling water. Constantan wires are spot-welded, one to the center and the other to the edge of the silver foil. A thermal emf is thus produced when heat flux is received by the silver surface. The radiometers used in this study were calibrated by NRDL personnel using a standard thermal radiation source. A radiometer, similar in operation to those used in this study, is described in Ref. 5.

During the flux measurements, the radiometer was so mounted in the CIT solar furnace that the receiving surface was in the equatorial plane of the lens hemisphere and moved with the furnace during the tracking of the sun.[4] The radiometer mounting made use of a standard Palmgren rotary table which allowed two 4-in. movements at right angles to each other. A third movement of the radiometer was possible through adjusting screws that effected movement perpendicular to the plane of the other two movements, toward and away from the sun.

The location of the maximum heat flux was first determined, and then the profile of the heat flux was obtained by traversing the radiometer across the image area. This was done for three cases: central lens only, central seven lenses, and all lenses operating.

RESULTS

(1) Flux Measurements at Sun Image

Preliminary experiments were made using one of the radiometers which had been described by the NRDL personnel as being possibly less reliable than the other. After gaining experience, two runs were made using the second radiometer. During the first of these, it was found that a slight adjustment toward the sun was necessary in order to obtain maximum flux readings when additional lenses were brought into operation.

This adjustment was made in each case for the final run, and, for this reason, these values are considered to be the most accurate. The thermal emf profiles across the sun image for the three cases are presented in Fig. 3 for this run. The integrated average thermal emf values over the sun-image area were obtained from these curves and were found to be 1.85 mv for the central lens, 7.28 for the central seven lenses, and 9.14 for all nineteen lenses. The maximum values were 2.25, 8.8, and 12.5 mv for the same three conditions, respectively.

At the end of the profile measurement, with all lenses operating during this last run, inspection of the radiometer revealed that the platinum-black coating had been partially removed. Apparently this had occurred during the latter part of the run when all the lenses were in operation. A recalibration by NRDL personnel indicated that the final calibration was 17.6 cal per sec per sq cm per mv in place of the original value of 13.5. Using the latter value for the profiles with the central lens open and with the central seven lenses open, the maximum and average values of the thermal emf can be converted to thermal flux

FIG. 3 — Thermal profiles in focal plane of California Institute of Technology solar furnace.

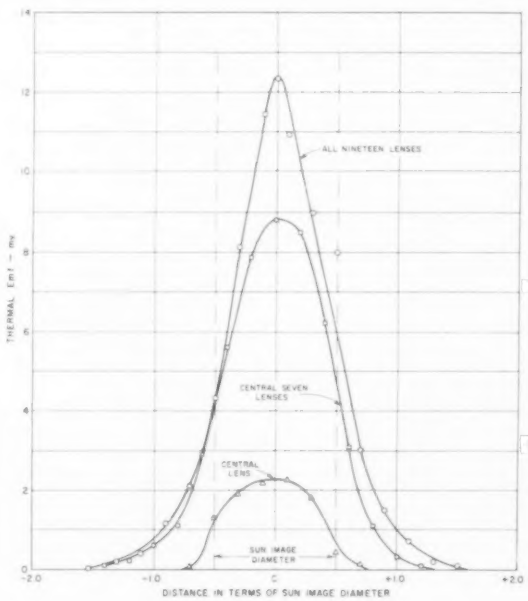

VOL. 1 1957

with the results given in Table I. Similarly, the higher calibration was used to obtain the results for all nineteen lenses open.

One interesting feature of Fig. 3 is that the flux values are far from uniform over the sun-image area. For the case where all lenses are in operation, the actual flux value at the edge of the "theoretical sun image" is only about one-third that at the center. This is in part due to the fact that the sun in reality is not a uniformly irradiating disk, but has a maximum radiation over the central portion.

These values of flux are for the case where the receiving surface is a plane surface, perpendicular to the direction of the sun, and they must be corrected, of course, if the receiving surface is a horizontal plane surface. This correction has been discussed in detail in the ASTIA document on which Ref. 4 is based. For example, the maximum values given in Table I would be reduced about 10 per cent in the case where the receiving surface is horizontal.

TABLE I

PERFORMANCE OF THE CALIFORNIA INSTITUTE OF TECHNOLOGY SOLAR FURNACE AT THE SUN IMAGE

A. Heat Flux Values

	Central Lens Open	Central Seven Lenses Open	All Nineteen Lenses Open
Maximum heat flux (cal/sec/sq cm)	30.4	119	220
Average heat flux over sun image (cal/sec/cm²)	25.0	98.3	161

B. Performance Characteristics

	Central Lens	Inner Seven Lenses Less Central Lens	All Nineteen Lenses Less Inner Seven Lenses
Direct solar radiation, normal to the sun, at the furnace site (cal/min/cm²)	1.04	1.04	1.04
Atmospheric transmission coefficient η_a (relative to solar constant of 1.98 cal/min/cm²)	0.525	0.525	0.525
Area concentration factor	2304	13824	27648
Concentration efficiency η_c	1.00	0.692	0.285
Theoretical concentration ratio	2304	9570	7880
Average flux at sun image (cal/sec/cm²)	25.0	73.3	62.7
Actual concentration ratio	1440	4230	3620
Fractional furnace efficiency	0.625	0.442	0.459
Lens efficiency	0.625	0.625	0.625
Mirror efficiency	None	0.707	0.734

Measured on August 15, 1956, from 2:00 to 2:40 pm, PDT

(2) Flux Measurements at Furnace Site

The total and sky radiation on a horizontal flat plate were recorded with an Eppley pyrheliometer during the time the flux measurements at the furnace focus were being made. The observed values of total radiation and direct radiation on a horizontal flat plate and the calculated values of direct radiation on a flat plate facing the sun are given in Table II. The direct radiation is that which can actually be concentrated by a solar furnace. For a clear day, this value will be fairly constant since it has already been corrected for the zenith angle of the sun. For August 14 and 15, it varied from 0.97 to 1.19 cal per min per sq cm. For a solar constant of 1.98 cal per min per sq cm, this indicates an atmospheric transmission efficiency η_a of 0.49 to 0.60.

TABLE II

SOLAR RADIATION DATA

(cal/min/sq cm)

Date	Time PDT	Radiation on Horizontal Plate			Direct Radiation on Flat Plate Facing the Sun
		Total	Direct	Fraction Direct	
8/14/56	1:30 pm	1.35	1.01	.75	1.08
8/15/56	10:25 am	1.16	0.91	.78	1.19
8/15/56	11:35 am	1.34	1.03	.77	1.16
8/15/56	1:05 pm	1.38	1.05	.76	1.12
8/15/56	3:10 pm	1.12	0.79	.70	0.97

(3) Calculation of Furnace Factors

The information on the flux profile in the focal plane and the available radiation at the site can be used to calculate some of the efficiency factors for this furnace.

The atmospheric transmission efficiency η_a is that portion of the solar radiation just outside of the earth's atmosphere that can be concentrated at the furnace site. This efficiency is affected not only by actual absorption by the air mass but also by water vapor, smog, and scattering of the light by fine particles. The actual radiation usable at the site is thus the direct radiation received on a flat plate facing the sun.

From Table II this can be interpolated to be 1.04 cal per min per sq cm on the average, during the period of the last run on August 15. Since the solar constant p_o is 1.98 cal per min per sq cm, the transmission coefficient η_a was 0.525.

Each of the lens arrangements were considered separately in determining optical efficiencies. In calculating these efficiencies the flux received on a flat plate facing the sun was used. Only the central lens of the nineteen lenses in the lens hemisphere produces a circular image or "sun image," on the equatorial plane, or in this case, on the radiometer face. The images from the other lenses are ellipses which increase in area inversely with cos θ, where θ is the azimuthal angle of each lens type.[1] On this basis, the central lens has a concentration efficiency η_c of 1.00, the six inner lenses with $\theta_A = 46.2°$, an η_c of 0.692. The outer twelve lenses, six with $\theta_B = 67.3°$, and six with $\theta_C = 79.4°$, have an average of η_c of 0.285.

The area concentration factor of the central lens is the ratio of the area of the 2-ft-diameter primary lens to the area of the ½-in. sun image, or 2304. The theoretical concentration ratio is this ratio times the concentration efficiency, or, in this case, still 2304.

The actual concentration ratio is the ratio of the actual flux over the sun image, 25.0 cal per sec per sq cm, to the direct radiation available at the site, 0.0173 cal per sec per sq cm (1.04 cal per min per sq cm) or 1440. The ratio of the actual to the theoretical is then the fractional

efficiency of the furnace, or, in this case, 1440/2304 or 0.625. The losses of 37.5 per cent are due to absorption in the glass lenses and to their geometrical imperfection.

The inner six lenses will have six times the concentration factor, but, since the concentration efficiency is only 69.2 per cent, due to the fact that the image from these lenses forms ellipses on a plate facing the sun, the theorectical concentration ratio will be 9570.

The flux contribution of these lenses can be obtained from the difference between the flux for the inner seven lenses, 98.3 cal per sec per sq cm, and the central lens, 25 cal per sec per sq cm, which is 73.3 cal per sec per sq cm. The actual concentration ratio then is 4230, resulting in a fractional furnace efficiency of 0.442. The lens losses are the same, so that the remainder of the losses are due to poor reflectivity and geometrical imperfection of the mirror system. This would be $1 - (0.442/0.625) = 1 - 0.707 = 0.293$ or 29.3 per cent losses due to the mirrors.

The same procedure may be carried out for the outer twelve lenses. Thus, the flux contribution of these lenses is 161 — 98.3 or 62.7 cal per sec per sq cm. The theoretical concentration ratio is $12 \times 2304 \times 0.285 = 7880$. The actual concentration ratio is 3620, giving a fractional furnace efficiency of 0.459. In the same manner as before, this leads to 26.6 per cent losses due to the mirrors. This checks quite well, since the efficiency of the outer twelve lens systems should be the same as for the inner six, considering that the losses for both systems are similar, involving two lenses and one mirror. These results are also summarized in Table I.

The same type of calculations can be made for the entire furnace. For all nineteen lenses operating, the area concentration factor is 43,800, and the concentration efficiency is 45 per cent,[1] so that the theoretical concentration ratio is 19,700. The average flux is 161 cal per sec per sq cm, which leads to an actual concentration ratio of 9,300 and a fractional furnace efficiency of 47.2 per cent. The losses of 52.8 per cent are ascribed to transmission losses in the lenses, reflectivity losses at the mirrors, the geometrical imperfection of the individual lenses and mirrors, and lack of perfect superposition of the nineteen images.

ACKNOWLEDGEMENTS

The authors wish to express their appreciation to the NRDL for the use of the radiometers. In particular, they express their thanks to Richard P. Day and Richard Hillendahl of the Thermal Radiation Branch of NRDL for their kind assistance.

REFERENCES

1. Hiester, N. K.; Tietz, T. E.; Loh, E.; and Duwez, P., "Theoretical considerations on performance characteristics of solar furnaces." *Jet Propulsion* 27:507, 1957.
2. Hiester, N. K.; Tietz, T. E.; and De La Rue, R. E., Jr., "Economic factors in furnace design." *J. Solar Energy Sci. Eng.* 1:28, April-July 1957.
3. Duwez, P. and Loh, E., "Phase relationships in the system zirconia-thoria." *J. Am. Ceram. Soc.* 40:321, 1957.
4. Hiester, N. K.; Loh, E.; and Tietz, T. E., "The operation and use of the California Institute of Technology lens-type solar furnace." ASTIA Document No. AD 88368 (AFOSR-TN-56-248), April 24, 1956. (To be published in the *Trans. of the Conference on the Use of Solar Energy — the Scientific Basis.* Tucson, University of Arizona Press.)
5. Gardon, Robert, "An instrument for the direct measurement of intense thermal radiation." *Rev. Sci. Instr.* 24:366, 1953.

VOL.
1
1957

A GUIDANCE SYSTEM FOR A SOLAR FURNACE

By JAMES G. MOORE and PIERRE ST. AMAND

Michelson Laboratory,
U.S. Naval Ordnance Test Station, China Lake, California

A guidance system for a solar furnace is described. The system will automatically track the sun about any two orthogonal axes. A single photosensitive detector is used in conjunction with a rotating shutter to generate an a-c error signal. The amplitude of the error signal is dependent upon the radial displacement of the solar image from the optic axis. The phase of the error signal is dependent upon the angular position of the image. The error signal is amplified and used to operate two motors which direct the seeking system so that the optical axis is pointed toward the sun.

INTRODUCTION

A guidance system for tracking the sun in azimuth and elevation or any other pair of orthogonal axes is described. The system uses a seeker, an amplifier, two two-phase servomotors and a 900-to-1 gear reductor to drive the original gear trains of a 5-ft antiaircraft searchlight of the type commonly adapted to solar furnace work.[1,2] The seeker is attached to the side of the solar furnace and is collimated with the optic axis of the searchlight mirror. When directed toward the sun, the system is capable of continuous tracking in both azimuth and elevation with an error of less than 1 minute of arc.

THEORY OF OPERATION

The seeker mechanism of the guidance system employs a single light-sensitive device to deliver an azimuth and elevation error signal to the servoamplifier and thence to the servomotors. The principle of operation is similar to that of the seeker in the sun follower for V-2 rockets described by H. L. Clark.[3] A photovoltaic cell is placed behind a semicircular shutter driven at 60 rps by a synchronous motor. The shutter is placed in the focal plane of the objective lens of the seeker telescope with its center of rotation coincident with the optic axis. A field lens casts an image of the objective onto the photovoltaic cell, thereby ensuring uniform illumination of the cell.[4] This prevents an error signal from being developed due to nonuniform sensitivity of the cell surface. Fig. 1 is a sketch of the seeker components.

FIG. 1 — A sketch of the seeker components. The telescope has an effective focal length of 9.23 in. and a field of view of approximately 4°. The detector is a photovoltaic cell (Natfab type S-1). An aperture, not shown, limits the amount of light impinging on the detector.

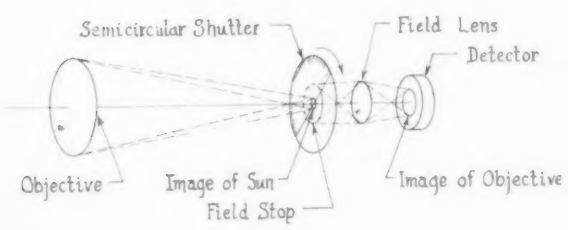

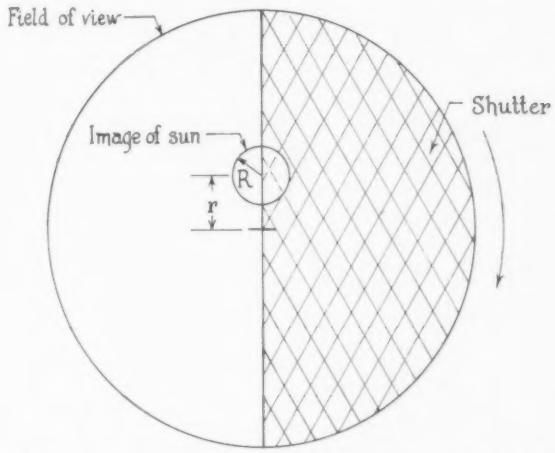

FIG. 2 — A scale drawing of the focal plane of the seeker telescope showing a displacement of the solar image from the optic axis and its relationship to the rotating semicircular shutter.

When the image of the sun is on the optic axis, the 60-cycle output of the cell is zero. However, when the image drifts off axis in any direction, a 60-cycle voltage is generated at the output of the cell. The amplitude $E(r)$ of the voltage is a function of the radial displacement r of the image while the phase θ_i of the voltage depends upon the angular displacement of the image from a reference direction. (See Fig. 2 and Fig. 3.) This reference direction is determined by the angular position ϕ of the shutter with respect to the phase position of the shutter-drive rotor and hence of the a-c line voltage. This voltage $E(r)$ is fed into the amplifier and appears as $\mu E(r)$ at the signal windings of the azimuth and elevation servomotors. Here μ

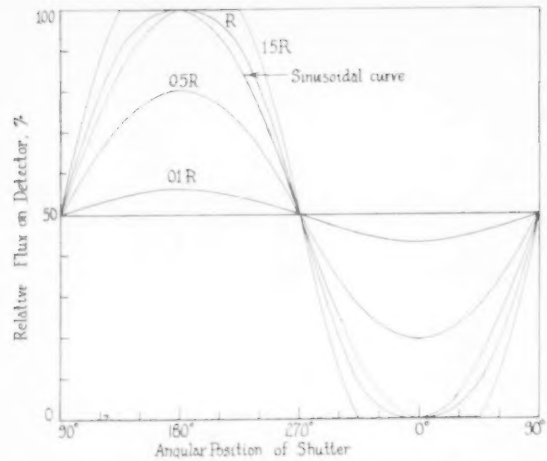

FIG. 3 — A graph showing the variation of light flux appearing at the detector as a function of image displacement and shutter position. Image displacement is in fractions of solar radii.

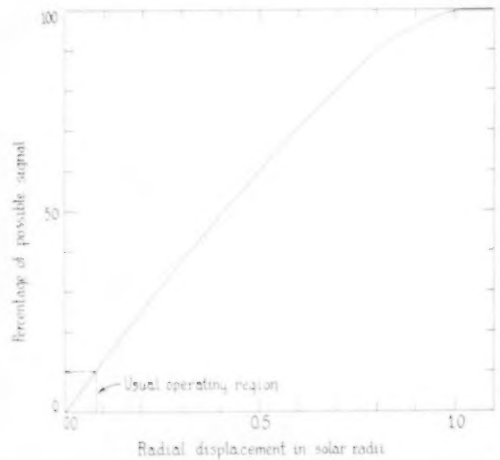

FIG. 4 — A graph of relative amplitude of the error signal as a function of image displacement. In the usual operating region, the error signal is a linear function of the radial displacement of the solar image.

represents the gain of the amplifier. Fig. 4 indicates the magnitude of $\mu E(r)$ as the image of the sun is allowed to drift off the optic axis of the seeker telescope.

The reference windings of these two-phase motors are phased 90 electrical degrees apart. The elevation reference winding is connected to the a-c line voltage. The azimuth reference winding is connected to the line voltage shifted through 90 electrical degrees by use of a condenser. The action of the servomotors is shown in Fig. 5, a voltage vector diagram. The component E_{s1} of the signal voltage effective in rotating the elevation motor will be $\mu E(r)$ sin θ_i. The component E_{s2} effective in rotating the azimuth motor will be $\mu E(r)$ cos θ_i. Rotation of the elevation and azimuth motors will be clockwise or counterclockwise depending upon the algebraic sign of E_{s1} and E_{s2} respectively.

The angular position ϕ of the shutter is adjusted by disengaging the shutter from the shutter-drive motor and mechanically rotating the shutter while thus disengaged. With an image of the sun on the optic axis and the elevation reference voltage off, the solar furnace is moved about its elevation axis and the shutter is oriented until E_{s2} is equal to zero. This ensures that an elevation error signal is not interpreted as an azimuth error signal by the tracking mechanism. Since the shutter-drive motor does not have a polarized rotor, it is possible for the shutter to start in either one of two positions, i.e., $\phi = 0°$ or $\phi = 180°$. If $\phi = 0°$, the furnace will track until E_{s1} and E_{s2} are both equal to zero. This occurs only when the image of the sun lies on the optic axis of the seeker telescope. This is the desired mode of operation. If $\phi = 180°$, the solar furnace will again track until E_{s1} and E_{s2} are both equal to zero. This occurs only when the sun is out of the field of view of the seeker telescope. This is the undesired mode of operation. It is easy to "slip a pole" in the 2-pole shutter-drive motor in order to select the desired mode of operation. This is done by turning the power switch off and on until the "slip" has been accomplished.

The amplifier consists of a power supply, a single amplifying stage, a phase splitter, and a push-pull output stage. It is also equipped with the necessary circuits to allow the operator to position the solar furnace so that

FIG. 5 — A vector diagram showing amplitude and phase relationships between azimuth and elevation servomotor voltages and the error signal voltage.

Phase Angle	Function of Voltage
0	Shutter reference, reference phase for elevation motor, signal phase for azimuth motor (clockwise rotation)
$\frac{3\pi}{2}$	Reference phase for azimuth motor, signal phase for elevation motor (counter-clockwise rotation)
π	Signal phase for azimuth motor (counter-clockwise rotation)
$\frac{\pi}{2}$	Signal phase for elevation motor (clockwise rotation)

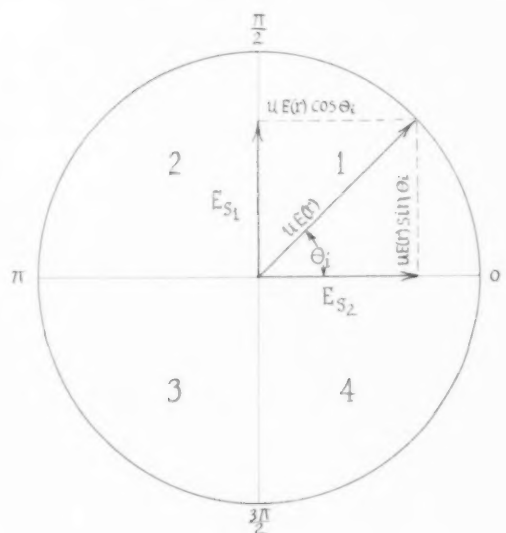

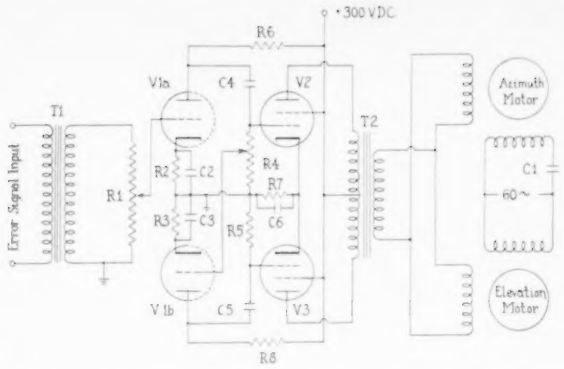

FIG. 6 — A simplified schematic diagram of the servoamplifier. The positioning control circuits and power supply have been omitted for simplicity.

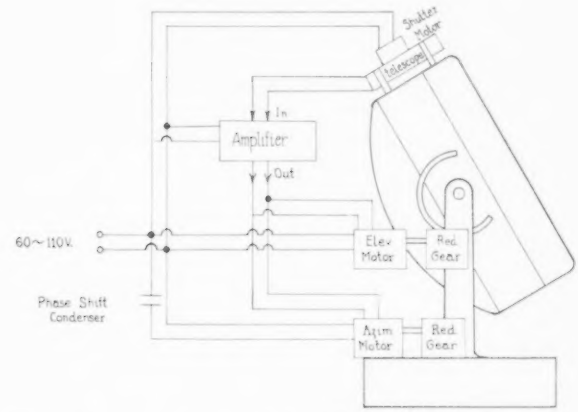

FIG. 7 — A block diagram of the solar furnace and guidance system.

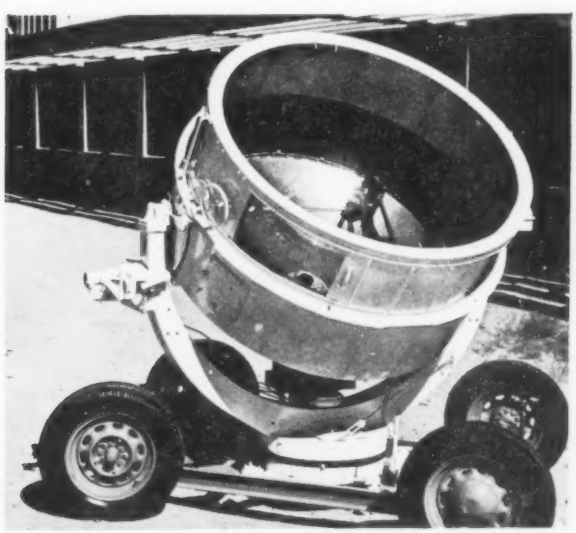

FIG. 8 — A photograph of the solar furnace. The servoamplifier may be seen on the yoke under the mirror holder. An observation port may also be seen in the center of the paraboloidal mirror. The furnace is mobile and only requires a 60 cycle-115v a-c source for operation of the guidance system.

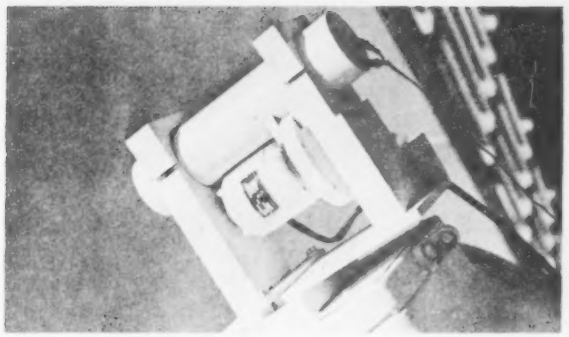

FIG. 9 — A photograph of the telescope, shutter-drive motor, and detector that comprise the seeker for the guidance system.

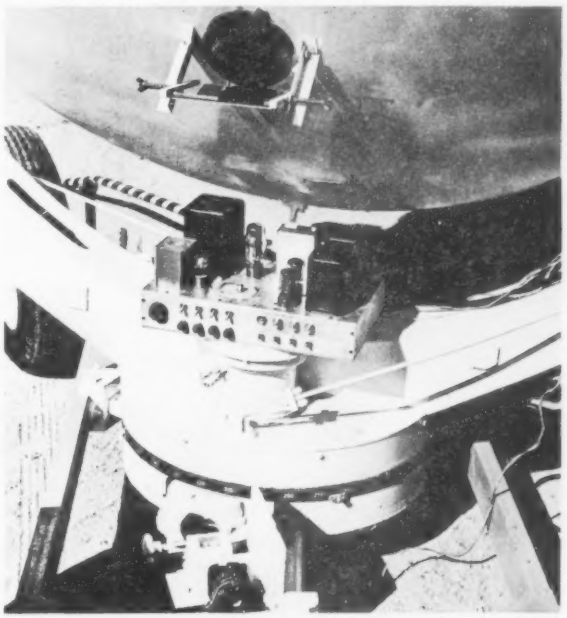

FIG. 10 — A photograph of the amplifier and azimuth drive system. Note the mirror and polaroid filter that enable the operator to view the sample held at the focus of the concentrator.

the sun appears in the field of view of the seeker telescope. A simplified circuit diagram of the amplifier is shown in Fig. 6. Fig. 7 is a block diagram of the solar furnace and guidance system. Fig. 8 is a photograph of the solar furnace. Fig. 9 is a photograph of the seeker and Fig. 10 is a photograph of the amplifier and azimuth drive system.

ACKNOWLEDGEMENTS

C. P. Pentoney and Z. W. Hohanshelt of the Physics Model Shop deserve special thanks for the fabrication of many essential parts used in the seeker and drive mechanisms.

REFERENCES

1. C. J. Kevane, "Construction and operation of the ASC solar furnace." *J. Solar Energy Sci. Eng.* 1(2-3): 99-101, Apr.-July 1957.
2. W. M. Tuddenham, "A solar furnace for research in nonferrous metallurgy." *J. Solar Energy Sci. Eng.* 1(2-3): 48-51, Apr.-July 1957.
3. H. L. Clark. *Electronics* Oct. 1950.
4. P. St. Amand. Thesis (Ph.D.) — California Institute of Technology, 1953.

SOLAR RADIATION DURING THE SOLAR ECLIPSE OF DECEMBER 14, 1955 AT COLOMBO, CEYLON

By P. SELVANAYAGAM and J. C. V. CHINNAPPA

University of Ceylon, Colombo

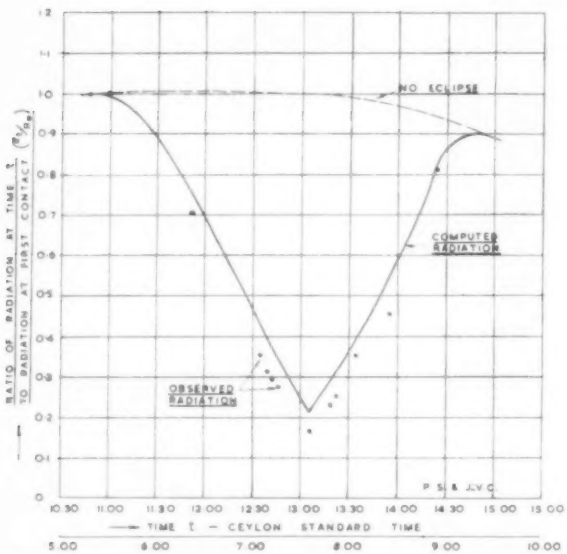

FIG. 1 — Solar radiation during eclipse on December 14, 1955.

Measurements were made with a Kipp pyrheliometer of the direct solar radiation at Colombo, Ceylon, during the solar eclipse of December 14, 1955. Recorded measurements are plotted as fractions of radiation observed at first contact and compared with the theoretical curve based on Briggs' equation.

Solar radiation measurements during a total solar eclipse were made in Brazil in 1947 by Lyman J. Briggs.[1] The authors took advantage of the partial eclipse (about ⅞) that was visible in the south of Ceylon on December 14, 1955, to take similar measurements. Though the number of observations obtained was limited, because of interference by clouds, it is felt that the results that have been obtained will perhaps be of some interest to other investigators.

A Kipp pyrheliometer was employed. This pyrheliometer measured only direct radiation from the sun and was sighted on the sun for each reading. The radiation measured was therefore direct solar radiation (with no radiation from the sky), normal to the receiving surface. The readings were made on a sensitive "Cambridge" galvanometer and allowances were made for resistances in the circuit. The observations were made at Colombo at about 8 ft above sea level.

The sky was clear of clouds before first contact. Shortly before first contact, patches of cumulus cloud were observed moving toward the sun, and these clouds interfered with observations after first contact. However, readings were taken whenever no cloud was seen to obscure the sun. These readings have been plotted as fractions of radiation observed at first contact.

The theoretical curve shown in Fig. 1 is based on Lyman J. Briggs' equation, viz:

$$\frac{R_t}{R_o} = A \times B \times \frac{\sin a_t}{\sin a_o} \times p^{(\sec Z_t - \sec Z_o)} \qquad [1]$$

where R_t = radiation received at time t
R_o = radiation received at first contact
A = fractional area of sun's disc not covered by the moon
B = correction factor to allow for variation of brightness of the solar disc as the limb is approached
a_t = altitude of the sun at time t
a_o = altitude of the sun at first contact
p = transmission coefficient of the atmosphere (taken as 0.75 at sea level)
Z_t = zenith angle at time t
Z_o = zenith angle at first contact

The above Equation [1] is for the vertical component of direct radiation from the sun received on a horizontal surface. The Eppley pyrheliometer used by Briggs measured the total radiation from the sun and the sky, and so Equation [1] is not strictly applicable to his observations. As the authors used a pyrheliometer which measured only direct radiation from the sun, Equation [1] reduces to

$$\frac{R_t}{R_o} = A \times B \times p^{(\sec Z_t - \sec Z_o)} \qquad [2]$$

The correction factor B was calculated using the method described by Briggs and using his figures for the relative brightness of the five circular zones of the sun's disc. The required astronomical data for the zenith angle at different times was obtained from the Nautical Almanac (1955).

It will be noticed that there is close agreement between the recorded measurements and the computed curve. The measurements made, however, are less than the theoretical

VOL. 1 1957

values, and this may possibly be due to the presence of haze difficult to observe.

ACKNOWLEDGEMENTS

The authors wish to express their thanks to Mr. T. Kidnapillai and Mr. M. S. Perera for their assistance in the calculations.

REFERENCES

1. Lyman J. Briggs, "Observed and computed radiation from first to fourth contact during a total solar eclipse." (To be published in the *Transactions of the Conference on the Uses of Solar Energy, the Scientific Basis*. Tucson, Univ. of Arizona Pr.)

OL.
1
957

SOLAR ENERGY IN SPAIN

By LEONARDO VILLENA

Instituto de Optica "Daza de Valdes", Madrid, Spain

From measurements made at the Optical Institute in Madrid, the energy on three specially orientated surfaces is calculated in the wavelength range 0.3 to 1.2 μ, including both the direct and the diffused radiation. Using measurements and observations made by the Astronomical Observatory in Madrid and keeping in mind the actual insolation time, the atmospheric absorption, and the inclination of the solar rays, the total energy coming directly from the sun in all wave lengths is calculated on the same surfaces. The first calculation gave a result, for the best orientated surface, of 1810 kwh per sq m per year, and the second calculation, a result of 1230 kwh per sq m per year. Therefore, the electrical energy that a silicon cell or a thermocouple with concentrating device could supply per year is 199 kwh per sq m or 37 kwh per sq m, respectively.

Madrid was selected for this study, not only because of the experimental facilities available, but also because the latitude, altitude, and sun hours per year for this city are close to the average over Spain. If we do not take into account the narrow strip along the Cantabrian and Pyrenees range of mountains, the average for this last factor varies between 2,500 and 3,200 hours per year over Spain, while in Madrid it is 2,890 hours.

FIG. 1 — Diurnal variation of the illuminance for the horizontal plane.

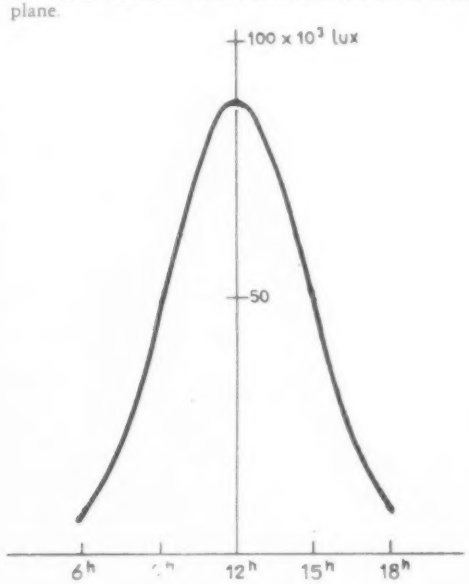

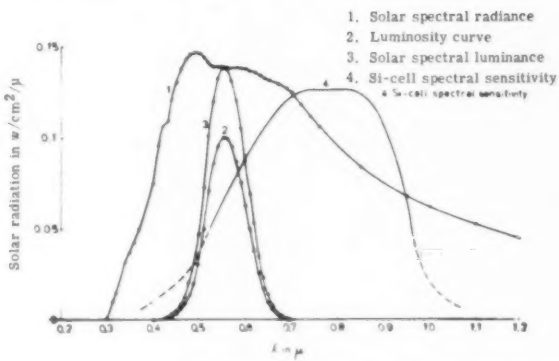

FIG. 2 — Spectral irradiance of the sun at the earth and its perception through the eye.

TOTAL RADIATION BETWEEN 0.3 AND 1.2 MICRONS

The experimental setup consisted of a Weber-type photometer, through which the illumination of various selected surfaces was measured at 9 a.m., noon, 3 p.m., and 6 p.m. From these measurements we selected those which correspond to a horizontal, south-orientated vertical, and an inclined plane, the normal of which is pointing each day to the sun at its maximum height. The average illumination at noon, taking into account all the days (cloudy and sunny) of the year is:

$$E_h = 88{,}000 \text{ lux}$$
$$E_v = 69{,}000 \text{ lux}$$
$$E_i = 94{,}000 \text{ lux}$$

From measurements at different times, average curves were plotted, as in Fig. 1, showing the daily variation of the illumination (influenced by the angle at which the solar rays hit the surface and the absorption produced by clouds and depth of the atmosphere). The mean values of these curves (referred to the noon illumination) are:

$$T_h = 0.56$$
$$T_v = 0.53$$
$$T_i = 0.55$$

If we are interested in knowing the solar energy which could be used by the new silicon cells, it is necessary to turn from illumination data to the amount of energy in

VOL. 1 1957

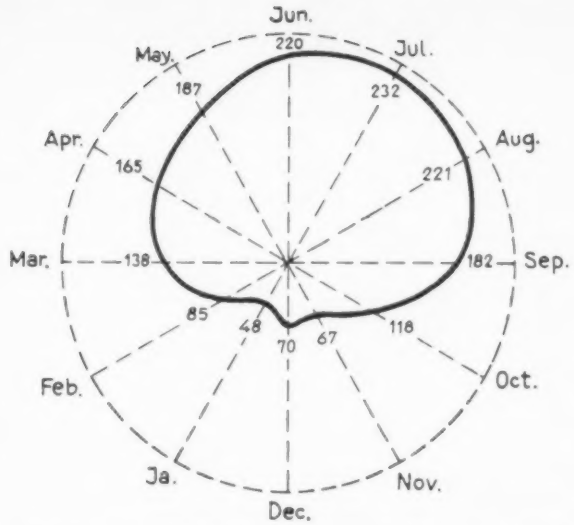

FIG. 3 — Monthly distribution of the energy (diffused and direct) received by the horizontal plane.

the wavelength range 0.3 to 1.2 μ. For this purpose we take into consideration (Fig. 2) the spectral distribution of the solar irradiation,* the eye response curve, and the product of both, from which it is deduced that instead of 1 w = 680 lumens (valid for the maximum sensitivity of the eye) we have to use 1 w = 262 lumens. Now the values so obtained have to be multiplied by a factor of 2.06, which is the ratio between the energy carried by the solar radiation in the visible range and in the 0.3 to 1.2μ ranges, which are used by the silicon cells.

Bearing all these factors in mind and using as total sun-hours per year the theoretical value of 4455 (thus meaning that we exclude the small amount of energy falling upon the earth during the crepusculae), we found that the total energy per year in kwh per sq m received by the horizonal, vertical, and inclined planes in the above-mentioned range, taking into consideration both the direct sun rays and the diffused radiation, is:

$$V_h = 1740$$
$$V_v = 1290$$
$$V_i = 1810$$

The variation of V_i through the months of the year is shown in Fig. 3.

SOLAR DIRECT RADIATION

We found it interesting to know also the amount of the radiation coming directly from the sun in all wavelengths. We started this calculation from the measurements made by the Astronomical Observatory in Madrid, which give as average value for sunny days at noon

$$Q = 12{,}300 \text{ cal/m}^2\text{/min.} = 860 \text{ w/m}^2$$

Also using the measurements made by the Astronomical Observatory on clear days, we drew the average curve of

*We used only the spectral distribution of the solar light in spite of the fact that on cloudy days some change in this spectral distribution has to be expected.

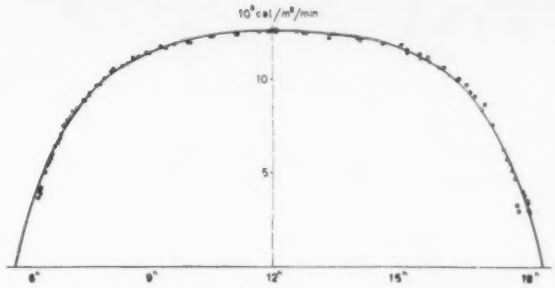

FIG. 4 — Diurnal variation of the energy received by a surface normal to the sun at the earth on clear days.

Fig. 4, which gives as a mean value of the received energy, as referred to the noon value,

$$T = 0.81$$

This means that during an equinoctial sunny day (12 hours duration) the total energy received by a surface which is continually pointing to the sun is

$$W = Q \cdot T \cdot 12 = 8.4 \text{ kwh/m}^2$$

This value is a little lower than the one found by Telkes (9.3 kwh per sq m).

We then needed to find the actual insolation time for each of the surfaces we selected, taking into account that the sun is not always seen from each of these surfaces and that it is hidden sometimes by the clouds. Fig. 5 was drawn from the data of the Meteorological Service to show the theoretical insolation time per year for the various vertical surfaces, together with the actual insolation time. It should be added that for the horizontal plane the theoretical insolation time is 4455 hours, and the actual time is 2890 hours, i.e., 65 per cent of the theoretical. The variation of

FIG. 5 — Summer insolation for vertical planes with different orientation. The thin line shows the theoretical insolation while the thick line refers to the actual one. The figures are a percentage of the insolation on the horizontal plane.

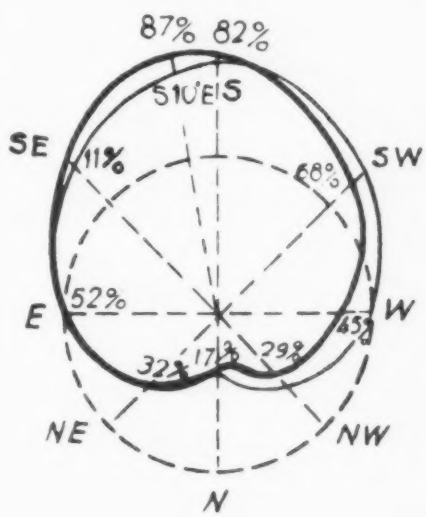

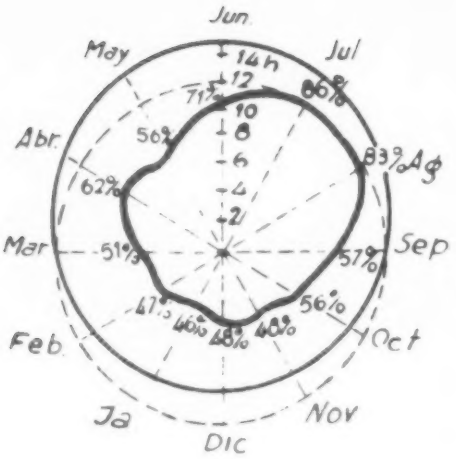

FIG. 6 — Insolation time by months of the year for a horizontal plane. The thin line shows the theoretical insolation while the thick line shows the actual one. The figures show the percentage of actual time compared with the theoretical.

the insolation time through the months of the year is shown in Fig. 6.

It is necessary to keep in mind the effect of the inclination of the solar rays on the different surfaces, as this varies during the day. The effect of the declination has been overlooked because it is self-compensated, provided the clouds at random are symmetrically distributed on both sides of the equinociae. For the first effect, remembering that the latitude of Madrid is 40° 25′, we have found as mean values of the correction coefficients for the three already-mentioned surfaces:

$$I_h = 0.48$$
$$I_v = 0.41$$
$$I_i = 0.64$$

In this way we found that the total direct energy falling on a surface which is continually pointing to the sun is, in kwh per sq m per year,

$$W = Q \cdot T \cdot 2890 = 2020$$

while for the horizontal, the vertical pointing to the south, and the inclined pointing every day to the maximum height of the sun, the total direct energy in kwh per sq m, is

$$W_h = Q \cdot T \cdot 2890\, I_h = 1000$$
$$W_v = Q \cdot T \cdot 2510\, I_v = 730$$
$$W_i = Q \cdot T \cdot 2770\, I_i = 1230$$

CONCLUSIONS

(a) Using a silicon cell with an efficiency of 11 per cent, it is possible to obtain as an average all over Spain 199 kwh per sq m per year, provided the panel is corrected each week to point at the maximum height of the sun.

(b) Using a concentrating device and thermocouple with an efficiency of 3 per cent, it is possible to obtain as an average all over Spain 61 kwh per sq m, provided the concentrating device is always pointing to the sun.

(c) The average thermal energy which can be obtained using a flat collector with an efficiency of 50 per cent is 500 kwh per sq m for a horizontal panel and a little more for a south-inclined one (depending on the inclination).

VOL.
1
1957

A SURVEY OF SOLAR FURNACE INSTALLATIONS IN THE UNITED STATES

SUPPLEMENT

Since the publication of the original survey of U.S. solar furnaces by Raymond K. Cohen and Nevin K. Hiester in the April-July 1957 issue of the *Journal*, details of four other furnaces have been received by the editor. These furnaces and their characteristics are listed below.

Organization	Sandia Corporation	University of Delaware	University of Delaware	University of Utah
Principal investigator	———	B. B. Chalabi M. H. Cobble	B. B. Chalabi M. H. Cobble	E. B. Christiansen
Furnace location	Albuquerque, N.M.	Newark, Del.	Newark, Del.	Salt Lake City, Utah
Date initiated	October 1955	March 1957	June 1956	June 1956
Furnace description, Main mirror:				
Mounting	Equatorial	Altazimuth	Altazimuth	Stationary
Mirror material	Bronze	Glass	Copper	Glass
Reflecting surface material	Aluminized with SiO_2 overcoat	Silver	Rhodium	Silver
Reflecting surface	Front	Back	Front	Back
Aperture	60 in.	60 in.	60 in.	60 in.
Focal length	26.5 in.	26 in.	26 in.	26 in. (approx.)
Rim angle	60°	60°	60°	———
Theoretical image diam.	0.231 in.	0.24 in.	0.25 in.	0.24 in.
Auxiliary mirrors & lenses				
No. of auxiliary mirrors	None	None	None	One
No. of lenses	None	None	None	None
System	Newtonian	———	———	Heliostat
Furnace operation, Guiding:				
Type	Clock drive with phototube corrector	Phototubes	Manual	Phototubes
Other details		Automatic suntracker	———	———
Temperature control:				
Type	None	Manual	Manual	Manual
Sensing device	———	———	———	Radiamatic pyrometer
Other details	———	———	———	Cylinder
Flux control:				
Type	Shutter ahead of focal plane	———	———	———
Sensing device	None	———	———	———
Other details	Preset timed shutter	———	———	———
Temperature measurements:				
Sensing device	Standard methods	Optical pyrometer & thermocouple	Optical pyrometer & thermocouple	Radiamatic pyrometer
Other details	———	———	———	———
Flux measurement:				
Type instrument	Flow calorimeter	———	———	None
Means for obtaining flux profile	Moon pictures	———	———	———
Other details	———	———	———	———
Specimen holder:				
Materials of construction	———	Titanium & kentanium	Steel & titanium	Carbon (graphite)
Type of traversing mechanism	3-dimensional	———	———	Screw
Applications & experimental results				
Use of furnace	Effect of high radiant energy flux rates on materials, part. as a step function (1/10 sec or faster)	———	———	Preparing specimens
Maximum temperature obtained	———	3000° C+	3000°C (approx.)	———
Maximum flux measured	———	———	———	———
Average local solar constant	1.4 cal/cm²/min	1.35 cal/cm²/min	1.35 cal/cm²/min	———
*Reflectivity efficiency factor	82% (est.)	———	———	80% (est.)
**Shadowing loss factor	92%	———	———	99% (est.)
General type of research	High temperature materials research	Performance measurement & heat transfer under high heat flux	Performance measurement & heat transfer under high heat flux	High temperature reaction and physical properties research (planned)

*Takes into account losses by reflectivity and/or absorptivity of all optical parts of furnace. (100 percent would denote no losses.)

**Takes into account losses due to shadowing of mirror by devices for mounting mirrors, targets, etc. (100 per cent would denote no shadowing.)

WORLD RESEARCH ACTIVITIES

The following survey of world-wide solar energy activities is intended to form a continuing current supplement to the directory section in *Applied Solar Energy Research* (Stanford Research Institute, 1955). As this section is a regular feature of the *Journal,* the editor will welcome any information on activities not mentioned below or in earlier issues, and on future developments in the utilization of solar energy.

AUSTRALIA

New South Wales University of Technology. Broadway, Sydney, N.S.W.

Is building a 12-ft diameter solar furnace made up of about 250 small mirrors and mounted on a 55-ft tower. It will be used for research on aluminum oxide and other refractories.

BURMA

Union of Burma Applied Research Institute. Junction of Kaba Aye Paboda-Kanbe Roads, Rangoon. Freddy Ba Hli; U Maung Maung; U Thaung.

Tested a number of different designs of solar cookers and sent a model of the most promising, a sectional aluminum reflector with a surface area of 18 sq ft, mounted on a light wooden frame and costing about 5 dollars, to the "Het Atoom" Exhibition in Amsterdam this summer. Conducted experiments on solar distillation using glass-roofed wooden boxes. Investigated the use of concentrated sulfuric acid for heat storage in connection with the solar cooker.

BELGIAN CONGO

Institut pour la Recherche Scientifique en Afrique Centrale. Lwiro, Bukavu.

L. van den Berghe, *director;* G. Bonnet; J. Cl. de Bramaecker; S. Guislain.

Operates a high-precision solar radiation laboratory recording direct, diffuse, and global radiation, as well as radiation in various spectral domains. Is building solar water heaters with techniques and materials suited to underdeveloped countries and has computed optimum area of collectors for various parts of the Congo. Will also build plastic solar cookers suited to underdeveloped countries. Is studying the effects of radiation, temperature, humidity, and ventilation on comfort factors in the design of houses.

EGYPT

University of Alexandria, Dept. of Mechanical Engineering. Alexandria.

M. Mamdouh Fikry.

Cooperating with the Desert Institute in the study of fresh water production, fruit drying, cooking, and power generation using solar energy. Postgraduate work on sea water distillation and salt production, and on optimum working pressures and temperatures for power generation with solar energy. Investigation of optimum designs of flat-plate collectors from the heat transfer and pressure drop points of view.

GERMANY

Köln Universität, Institut für Gärungswissenschaft und Enzychemie. An der Bottmühle 2, Köln.

Hermann Fink, *director.*

Studying the food and feed value of the unicellular algae *Scenedesmus obliquus* by experiments on albino rats and by chemical examination. Determined vitamin E and vitamin B_{12} factors (with Dr. Lundin of Stockholm), and investigated changes during the drying process of algae. 1500 single yields of algae were cultured at the Kohlenstoffbiologischen Forschungsstation in Essen. Animals examined histologically in cooperation with Dr. Eger of the Pathologischen Institut der Universität Göttingen.

LEBANON

Adnan Tarcici. c/o Yemen Legation, Alhamra Street, Beirut.

Has developed several solar cookers and is now working on a more compact, collapsible cooker for possible commercial manufacture.

SPAIN

Universidad de Madrid, Laboratorios de Electricidad y Electrónica. Madrid.

J. Balta.

Investigating the use of binary alloys as a substitute for silicon in solar batteries. Collected data on solar radiation and insolation in Spain and Canarian Islands during this century.

UNITED STATES

Arizona, University of, Institute of Atmospheric Physics, Tucson, Ariz.

A. R. Kassander, *director;* Raymond Bliss, Jr.

To design and build a house heated and cooled with solar energy, which will hold the Institute's solar radiation-measuring equipment.

George O. G. Löf Consulting Engineering Firm. 511 Farmers Union Bldg., Denver 3, Colo.

George O. G. Löf; Dale A. Fester; Harry Hawkins.

VOL.
1
1957

Completed solar-heated Denver House, a project in cooperation with the American Window Glass Co. of Pittsburgh, which utilizes overlapped glass flat-plate solar heat collectors and pebble beds for heat storage. In cooperation with the U.S. Office of Saline Water, designed a pilot plant for the solar distillation of sea water, to be built this year in the San Diego area. Carried out a program in cooperation with the University of Wisconsin involving the development of a plastic solar cooker and its preliminary field testing in Mexico, a study and evaluation of two types of intermittent absorption refrigeration units and their modification and improvement, and a limited study on black coatings. Made design improvements in a folding type of solar cooker for recreational use and built several models. Commercial manufacture under investigation.

New York University, College of Engineering, Solar Energy Laboratory. New York 53, N.Y.

Maria Telkes, *director.*

Designed solar cooking ovens using plane reflectors to augment energy received in an insulated oven, covered with transparent panes. Temperatures in excess of 400°F have been attained, sufficient for the preparation of most foods. (Sponsored by the Ford Foundation.) Built flat, tilted, and multiple-effect solar stills and operated them with sea water. (In cooperation with U.S. Office of Saline Water.) Studied selective black coating for solar heat collectors.

OL.
1
957

SOLAR ABSTRACTS

This section brings to the attention of our readers some of the important books and papers on solar energy which have been published elsewhere during the past few months. Wherever possible, authors' abstracts have been used; other abstracts are from the standard abstract journals or are by the editorial staff of the *Journal*. Photocopies of papers abstracted below may be obtained at cost (10¢ per page) by members of the Association for Applied Solar Energy, from the Association's library at Phoenix.

* * *

Anon., "Solar collector is source and sink for Japanese heat pump system." *Air Cond. Heat. Vent.* 54(8): 97-99, Aug. 1957.

Chiefly pictures, this article describes a heat pump system in Tokyo, Japan, at the home of the designer, Masanosuke Yanagimachi, which utilizes a solar collector as heat source in winter heating and heat sink in summer cooling.

* * *

Bremaecker, J. Cl. de, "Chauffe-eaux solaires." (Solar water heaters.) *Acad. Roy. Sci.Colon.* 2(3): 462-76, 1956.

The yearly cost of solar water heaters with auxiliary electric resistance is the sum of the amortizement and the electricity used. The latter expense can be expressed as a function of the minimum number of kcal per sq m per day (E) necessary to heat the water. A formula gives the optimum E depending on the radiation data of the area, the cost per sq m of the absorber (k), the expense of amortizement, and the price of the kwh (ϵ). From this, the area of the absorber, the yearly cost, and the initial expense are deduced and are shown by graphs as a function of k and ϵ for Lwiro (Bukavu, Belgian Congo). A general survey of types of absorbers is given in the addendum. (author's abst.)

* * *

Brooks, C. E. P., "Annotated bibliography on solar relations with weather." *Meteor. Abst.* 8(1): 95-119, Jan. 1957.

Lists works dealing wholly or in part with the effects of solar radiation on weather at the earth's surface and published during the period from about 1924 or 1925 to date.

* * *

Calvin, Melvin and Sogo, Power B., "Primary quantum conversion process in photosynthesis: electron spin resonance." *Science* 125(3246): 499-500, March 15, 1957.

The method of electron-spin resonance was used to observe changes during the early processes of photosynthesis. The appearance of a light-induced electron spin signal gave rise to investigations to determine the source of the signal. It appears that the signal is produced by the product of a physical process only, not an enzymatic or chemical one, and indications are that the signal is produced by a trapped electron or results from a dissociated bond. Chloroplasts are thus seen to have some of the properties of a semiconductor, and the photosynthetic process in plants to resemble in its primary stages the mechanism of the solar battery. *(Phys. Abst.)*

Courvoisier, Peter, "The solar engine: an analysis." *Mech. Eng.* 79(5): 445-47, May 1957.

A theoretical analysis of the solar engine, using the technique of the analog circuit to find the amount of power available from a given input of radiant energy. Formulae are derived which can be used to design solar engines. Illus.

* * *

Daniels, Farrington, "Chemistry and world energy needs." *Chem. Eng. News* 35:14-19, April 29, 1957.

Discussion of the role of the chemist in developing the production and use of atomic and solar energy. With regard to the utilization of solar energy, the following aspects are suggested for investigation by chemists: new materials and designs for a more efficient steam engine, needing only a small collector area to run on solar energy; cheap electrochemical systems for storing solar-generated electricity; methods for storing the hydrogen produced from water by a solar engine and a dynamo; methods for storing heat in solar space-heating systems; chemical systems for solar cooling; discovery of an endothermic photochemical reaction, using sunlight, in which the products can be stored indefinitely for use as fuel; reducing the cost of the solar battery by using polycrystals instead of a single large silicon crystal.

* * *

Drummond, A. J., "A contribution to absolute pyrheliometry." *Quart. J. Roy. Meteor. Soc.* 82(354): 481-93, Oct. 1956.

The results are presented of comparisons made in Southern Africa, during the years 1951-1954, between pyrheliometers of the Angström type which had been standardized at Davos (Switzerland), Leopoldville (Belgian Congo), Pretoria (South Africa), and Stockholm (Sweden). A section is also devoted to an investigation into the relationship between the original Angström scale and that embodied in the Abbot pattern of actinometer of the Smithsonian Institution, Washington. This latter series of comparisons was made at Pretoria (altitude 1370 m), under normal conditions of cloudless sky with reasonably steady atmospheric transmission.

The program was extended to include a comparison between specimens of these two substandard radiometers, using a controlled laboratory source of radiation. In these conditions, the radiometers were found to agree to within one-half per cent. This is further evidence of the small divergence (first pointed out by Guild in 1937) of the scale originated long ago by Knut Angström from the true standard of radiometry. (author's abst.)

* * *

Duwez, Pol, "Utilization of solar furnaces in high-temperature research." *Trans. ASME* 79(5): 1019-23, July 1957.

This paper presents a theoretical discussion of the performances of a parabolic-type solar furnace. Maximum temperature and maximum heat flux attainable at the focus are presented for furnaces of different diameter-to-focal-length ratios. It is shown that the optical quality of the parabolic reflector is the most important factor for obtaining high heat fluxes. With present-day technology, the heat flux is limited to 600 Btu per sq ft per sec, but this figure could be raised to 2300 Btu per sq ft per sec by improving the optics. Illus. (author's abst.)

* * *

Farber, Joseph and Davis, Burton I., "Analysis of large

VOL.
1
1957

aperture parabolic mirrors for solar furnaces." *J. Opt. Soc. Am.* 47(3): 216-20, March 1957.

An analysis is made of large aperture parabolic reflectors as solar furnaces to determine the most effective areas and estimate maximum attainable temperatures for two types of radiation targets. The maximum attainable temperature calculated is 5200° K. (authors' abst.)

* * *

Fritz, Sigmund, "Solar energy on clear and cloudy days." *Sci. Mo.* 84(2): 55-65, Feb. 1957.

An examination of the principal absorptions and scatterings that solar energy undergoes in its course through our atmosphere and a discussion of the spectral, geographic, and seasonal distribution of the energy that reaches the earth's surface. Based on a paper given at the Tucson Conference on Solar Energy — the Scientific Basis, Oct.-Nov. 1955. It is shown that in a cloudless atmosphere our knowledge of Rayleigh scattering and absorption by ozone permits fairly good engineering approximations of the average solar energy received at the ground on any surface at any time in almost any place, at least from the direct beam. The introduction of "dust" and water vapor require modification which can be taken into account when their amounts are known. In highly polluted atmospheres, the computations will become more difficult because of our imperfect knowledge of the number, size distribution, and the scattering and absorbing properties of the polluting particles.

Difficulties are encountered in computing the influence of clouds because they are inhomogeneous, and the theory has been simplified to take account of homogeneous clouds only. Also, not enough is known about drop-size distribution and the number of drops per unit volume in a given cloud. It is necessary to use empirical relationships between cloud amount indexes and solar radiation to estimate how much solar radiation will reach the ground on an average at a place where radiation measurements are not available. (author's summary)

* * *

Halacy, D. S., Jr., *Fabulous fireball; the story of solar energy.* N. Y., Macmillan, 1957. 154 p.

Intended for students on about the high-school level, this book describes the various ways in which solar energy is being and may be utilized. Following a brief historical survey, each chapter is devoted to one aspect of solar energy utilization: cookers, furnaces, air conditioning, algae culture, distillation, engines and power plants, photoelectric converters, photochemical processes, and solar-powered space ships. One chapter discusses opportunities for work in the solar energy field, and the book concludes with a description of solar energy utilization in a hypothetical town in the year 2050. Illus.

* * *

Hiester, Nevin K.; Tietz, Thomas E.; and Loh, Eugene, "Theoretical considerations on performance characteristics of solar furnaces." *Jet Propulsion* May 1957: 507-13, 546.

The theoretical factors affecting the performance of the parabolic-type solar furnace are discussed. Calculations of the heat flux and the maximum temperature obtainable at the focus are presented for furnaces of different diameter-to-focal-length ratios. The analysis is extended to the California Institute of Technology lens-type furnace. The results indicate that a paraboloid of relatively low quality is capable of achieving temperatures over 2000°K. On the other hand, a research furnace capable of attaining temperatures in the range of 3600 to 4200°K would have to have a paraboloid of very high quality. (authors' abst.)

* * *

Hutchinson, F. W., "Solar heating design procedure." (In his: *Design of heating and ventilating systems.* N. Y., Industrial Pr., ©1956. p. 238-88.)

Data for systems designed to make partial use of solar heating through the employment of large picture windows. Includes discussions of solar mechanics and heating effect, the instantaneous thermal advantage of a solar window, seasonal saving through solar heating, performance of solar windows, geometry of overhang design, and graphical design procedure for solar overhang. A number of graphical solutions are given for the more important equations in the chapter. Illus.

* * *

Jordan, R. C., "Here's why solar heating lags." *Heat. Pip. Air Cond.* 29(7): 111-14, July 1957.

Future energy requirements and possible sources are evaluated. The prime deterrents to the use of solar energy are the large capital investments required, the problem of integrating the collector into building architecture, and the relative abundance of fossil fuels at the present time. The heat pump and the adaptation of solar energy as a heat pump source are considered, and new developments in collector surfaces are discussed. Illus.

* * *

Masson, H., "Les insolateurs à bas potentiel (étude théorique et expérimentale). (Low temperature insolators; theoretical and experimental study.) *Chaleur et Industrie* April 1956. 28 p.

The collection of solar energy is especially interesting in arid areas where insolation is strong. Concentration systems, however interesting, are expensive. Moreover, they need very careful maintenance. Consequently, it has proved convenient to direct research work in arid areas towards low potential insolators. The author has tried to build up a theory for this kind of insolator, and to experiment systematically on the various types under investigation. It appears that the application of the theoretical formulae leads to the knowledge of the limits and possibilities of a given apparatus by the determination of a limited number of factors. Thus, the problem of rentability is easier to resolve. Illus. (author's abst.)

* * *

New Delhi Symposium on Wind and Solar Energy, Oct. 1954, *Wind and solar energy; proceedings of the New Delhi Symposium: Energie solaire et éolienne; actes du colloque de New Delhi.* Paris, UNESCO, 1956. 238 p. (Arid zone research 7.)

Proceedings of the symposium held at the National Physical Laboratory of India, under the sponsorship of the UNESCO Advisory Committee on Arid Zone Research and the National Institute of Sciences of India. In all, 22 papers are included, in the original language of their presentation, either English or French, with a summary in the other language and in Spanish, together with some account of the discussions. Authors represented in the solar energy section are: E. W. Golding and M. S. Thacker, F. Daniels, J. N. Black, A. E. H. Bleksley, V. A. Baum, Félix Trombe, H. Masson, L. A. Ramdasand, S. Yegnanarayanan, K. N. Mathur and M. L. Khanna (2 papers), A. L. Gardner, N. W. Pirie, and M. Beau. Illus., with subject index.

* * *

Stead, William H., "The sun and foreign policy." *Bull. Atomic Sci.* 13(3): 86-90, March 1957.

A general discussion of the use of solar energy vs. atomic energy as a supplemental source of energy, particularly for the economically underdeveloped nations. The author suggests that the United States should launch a major cooperative international program of solar energy research and development in an effort to help improve the standard of living in underdeveloped nations.

* * *

United Nations, Dept. of Economic and Social Affairs, *New sources of energy and economic development: solar energy, wind energy, tidal energy, geothermic energy and thermal energy of the seas.* New York, 1957. 150 p.

A report prepared by the UN Secretariat for the Economic and Social Council on the practical utilization of these five energy sources, taking into account the present state of knowledge and foreseeable future development, with special emphasis on benefits

to underdeveloped countries. It is based on research undertaken by the Secretariat and on background studies by five specialists, one in each of the "new energy" fields. The background study on solar energy was written by Farrington Daniels.

The first part of the report is a comparative study of the five energy sources, including characteristics, methods of utilization, possible use for the production of electric power and in other fields, and suggested lines of developments. The second part contains five studies, one on each of the sources under review, extracted from the background papers. The chapter on utilization of solar energy deals with the various methods of applying solar energy, considers its use as heat and as light, and discusses the economic aspects and limitations. This latter section points out the difficulties involved in storage costs, changing cultural patterns, availability of land, and climatic limitations on the use of solar energy. Illus. with annotated bibliography.

* * *

Von Allmen, Erwin *et al. Space conditioning with solar energy*. By Manufacturing Group No. 4, Erwin von Allmen *et al.* Report submitted in partial fulfillment of the requirements in Professor Doriot's course in Manufacturing at the Harvard Business School, during the academic year 1956-1957, April 1957. 71 p.

Intended to present a comprehensive picture of solar space conditioning from the laboratory to the market place. It provides an historical background for the present situation in the field of solar heating and cooling, a survey of the general energy-cost situation, an estimate of the regional technical-economic potential for this country, consideration of the current technical status, a survey of the industry in which it must compete, and a review of the miscellaneous economic and other factors which will influence the ultimate degree of acceptance at the consumer level. Illus.

VOL.
1
1957

ERRATA & ADDENDA

"Solar radiation availability on surfaces in the United States as affected by season, orientation, latitude, altitude, and cloudiness" by C. F. Becker and J. S. Boyd, in Vol. I, No. 1, Jan. 1957, p. 13-21: The procedure used for determining the cloudless-day solar radiation availability for sea-level conditions closely parallels that used by Threlkeld and Jordan (Ref. 16) and Hutchinson (Ref. 8 and *Heat Pip. Air Cond.* 21:102-4, 1949.)

* * *

"World research activities" in Vol. I, No. 1, Jan. 1957, p. 55: Under Arizona State College, Rocky Mountain Forest & Range Experiment Station, Tempe, Arizona, John P. Decker should be listed as a staff member, not director.

* * *

"Temperature and flux vs. geometrical perfection" by Tibor S. Laszlo, in Vol. I, No. 2-3, Apr.-July 1957, p. 82: The equation

$$\gamma = \frac{P_{calc}}{P_{meas}} = 76 \text{ per cent}$$

should read

$$\gamma = \frac{P_{meas}}{P_{calc}} = 76 \text{ per cent}$$

OL.
1
957